



HAL
open science

Geomagnetic field intensity at Hawaii for the last 420 kyr from the Hawaii Scientific Drilling Project core, Big Island, Hawaii

Carlo Laj, Catherine Kissel

► **To cite this version:**

Carlo Laj, Catherine Kissel. Geomagnetic field intensity at Hawaii for the last 420 kyr from the Hawaii Scientific Drilling Project core, Big Island, Hawaii. *Journal of Geophysical Research: Solid Earth*, 1999, 104 (B7), pp.15317-15338. 10.1029/1999JB900113. hal-03118601

HAL Id: hal-03118601

<https://hal.science/hal-03118601>

Submitted on 22 Jan 2021

HAL is a multi-disciplinary open access archive for the deposit and dissemination of scientific research documents, whether they are published or not. The documents may come from teaching and research institutions in France or abroad, or from public or private research centers.

L'archive ouverte pluridisciplinaire **HAL**, est destinée au dépôt et à la diffusion de documents scientifiques de niveau recherche, publiés ou non, émanant des établissements d'enseignement et de recherche français ou étrangers, des laboratoires publics ou privés.

Geomagnetic field intensity at Hawaii for the last 420 kyr from the Hawaii Scientific Drilling Project core, Big Island, Hawaii

Carlo Laj and Catherine Kissel

Laboratoire des Sciences du Climat et de l'Environnement, CEA-CNRS, Gif-sur-Yvette, France.

Abstract. Four hundred twenty five new paleointensity (Thellier-Thellier) determinations (out of 545 analyzed samples) have been obtained from core HSDP, which penetrates about 1000 meters (208 flows) of the Mauna Loa and Mauna Kea volcanic series encompassing the last 420 kyr. Rock magnetic investigations identify pseudo-single-domain magnetite as the main magnetic mineral. Inclinations are shallower than expected from a geocentric dipole field but are consistent with data from other geographical regions at the same latitude. The inclination record reveals three episodes of negative inclination whose interpolated age correlates well with that of known geomagnetic events. The paleointensity record from the Mauna Loa sequence is not very detailed and does not allow precise comparison with other data in the 0-50 kyr interval. The record from the Mauna Kea sequence, on the contrary, is very detailed and documents relatively short-lived episodes of low and high field strength from 15 to 60 μT . The average virtual dipole moment ($8.7 \pm 3.0 \cdot 10^{22} \text{ A}\cdot\text{m}^2$) is not significantly different from the value reported by *Kono and Tanaka* [1995] for the last 2.5 Myr. A comparison with other data from Hawaii and other geographical regions is described in detail. There are no drastic changes in paleointensity with the inclination anomaly, in agreement with previous results from Hawaii but in contrast with most published results which, however, consider data from polarity transition. Spectral analysis of a particularly detailed portion of the record, between 420 and 326 kyr, documents significant periodicities at 36, 8, 5, and 4 ka in the inclination record but not in the intensity record, suggesting that changes in time of the inclination are to a certain extent independent from those of the intensity.

1. Introduction

The 1 km core obtained near Hilo (latitude $19^{\circ}45'N$; longitude $-155^{\circ}05'$) by the Hawaii Scientific Drilling Project (HSDP) [*Hawaii Scientific Drilling Project*, 1994] penetrates 227 units of the Mauna Loa (43) and Mauna Kea (184) sequences. The main objective of HSDP is to drill continuously through a sequence of lava on the flank of the Mauna Kea volcano to obtain a stratigraphic sequence representing the complete traverse of the Hawaiian hotspot [*Stolper et al.*, 1996]. In addition, this core provides a unique opportunity to obtain a detailed record of geomagnetic field changes during the last 400 kyr from a continuous sequence of lava flows from the central Pacific.

Although the HSDP core is not azimuthally oriented, the records of the inclination and of the paleointensity may address several important issues relative to geomagnetic field behavior. The inclination record, for instance, has revealed two brief inclination reversals, which were tentatively correlated to the Blake and Jamaica events, and an anomalous inclination which was associated with the Laschamp event, all of which represent the first records of these events from the central Pacific, providing evidence for their worldwide character [*Holt et al.*, 1996]. In addition, long term variations

of the geomagnetic field are recorded in the inclination record, and the short-term characteristics appear to be superimposed upon these long-term trends.

Paleointensity determinations, which are among the most time consuming of all the paleomagnetic measurements, have not progressed as fast as the inclination measurements, and only a preliminary paper has been published so far [*Garnier et al.*, 1996]. With respect to sedimentary records, volcanic records of paleointensity have the great advantage that the processes by which the magnetization of a lava was acquired are relatively well understood and can be reliably reproduced in the laboratory. It is therefore possible to obtain determinations of the absolute field intensity by comparison with a known field in the laboratory, whereas the complicated nature of sedimentary magnetization only allows relative changes of the field intensity to be retrieved from sediments. Moreover, volcanic records do not suffer from possible environmental factors and from the time-averaging effect inherent to sedimentary acquisition of remanence. Therefore, despite their discontinuous nature, volcanic records may allow a better quantitative appraisal of geomagnetic field changes in the past than many sedimentary records do.

In this paper we report on 545 paleointensity measurements made on samples from core HSDP. The unusually high percentage (~75%) of successful determinations makes the HSDP record the longest continuous volcanic record of geomagnetic field intensity yet reported and allows some general conclusions about geomagnetic field behavior to be made.

Copyright 1999 by the American Geophysical Union.

Paper number 1999JB900113.
0148-0227/99/1999JB900113\$09.00

The $^{40}\text{Ar}/^{39}\text{Ar}$ and K/Ar datings from different horizons in the core [Sharp *et al.*, 1996] and one radiocarbon date of humic ashy soil [Beeson *et al.*, 1996] provide the necessary time constraints for the interpretation of this record in terms of geomagnetic field behavior.

2. Core Description and Sampling

The core logging [Stolper *et al.*, 1996] identified 227 units (numbered in stratigraphic succession from the top to the bottom of the core), out of which 208 are lava flows. The other units consist of ash beds, marine and beach sediments, and soils [Stolper *et al.*, 1996]. The upper 43 units (27 of which are lava flows) belong to the Mauna Loa volcano, and the lower 183 lava flows (flow numbers 44 to 227) belong to the Mauna Kea volcano. Mauna Loa lavas erupted on gentle slopes, while Mauna Kea lavas erupted on steeper slopes (3° to 6°) [DePaolo and Stolper, 1996]. As a result, Mauna Loa flows are thicker than those from deeper levels. The contact between these two series, at a depth of 279.5 m, is sharp and unambiguously identified by changes in trace elements ratios [Hofmann and Jochum, 1996; Rhodes, 1996] and He, O, Sr, Pb, and Nd isotopic ratios [Eiler *et al.*, 1996, Hauri *et al.*, 1996; Lassiter *et al.*, 1996].

No intrusive unit has been identified, and nearly all the lavas are subaerial [Stolper *et al.*, 1996]. The presence of subaerial lavas at 1 km depth is consistent with the subsidence rate of 2.0-2.5 mm/yr at Hawaii [Moore, 1987; Moore *et al.*, 1996] and the age of the bottom of the core (~ 420 kyr, see section 4). The choice of the drill site, where the effect of hydrothermal solutions was predicted to be minimal, has resulted in the recovery of remarkably fresh lavas. (Core description is available on the HSDP World Wide Web site http://expet.gps.caltech.edu/Hawaii_project.html)

For the paleointensity study, usually three (but in a few cases two or even one) samples were drilled in 190 flows (22 from Mauna Loa, 168 from Mauna Kea) within the working half of the HSDP core using a diamond-tipped, water-cooled coring bit in the core repository at the California Institute of Technology (Caltech). A vertical orientation line was drawn on the flat side of the core split parallel to the side of the core, and samples were then drilled centered on this line and perpendicular to the core axis. Care was taken to distribute the samples over the entire thickness of the flows. In general, the azimuths of the subsamples have no meaning due to the azimuthally unoriented nature of the core, but when continuous sections of the core were encountered, samples were drilled with the same azimuth. A total of 545 samples were obtained for paleointensity determinations. Samples were labeled by the number of the flow, followed by a letter identifying the different samples in the flow. Orientation marks were drawn on each sample, before being trimmed into one to three 12 mm subsamples, i.e., half the size of a standard paleomagnetic sample. End chips were used for rock magnetic analyses.

At the time of the sampling, we were not aware that a section of the core, spanning parts of flow units 199 and 200, had been inverted during core retrieval. This caused some changes in sample identification. As a consequence, we have no samples in flow unit 199, and we have six samples in flow unit 200.

During drilling of the core, flow unit 64 was recovered in

three separate sections. The samples used in this study and those used in the study of Holt *et al.* [1996] come from two different sections. For reasons discussed below, the possibility that one section has been inverted has recently been rechecked by J. W. Holt *et al.* (personal communication, 1998). Unfortunately, there is nothing to indicate whether the 3-foot section from which our samples come has been inverted or not. The section could be inverted and the lithological variation would match just as well as they do in its present position. There is no evidence either that the section of the core used for the Thellier experiments is part of a separate flow. There are crumbly sections of altered rock both above and below the fresh unaltered rock where the samples are from, but there is nothing that looks like a flow boundary (J. W. Holt *et al.*, personal communication, 1998).

3. Methods of Measurements

High field thermomagnetic analyses were made on small amounts of powder using a horizontal Curie balance in an argon atmosphere to minimize oxidation of the magnetic minerals during the experiments. Heating and cooling rates were close to $7\text{-}8^\circ\text{C}/\text{min}$, and the maximum temperature reached was 680°C in fields of the order of 0.4-0.9T. The S ratio, defined as $S = \text{IRM}(-0.3\text{T}) / \text{IRM}(1\text{T})$ [King and Channell, 1991], was determined on small chips of rock using an alternating gradient force magnetometer (AGFM).

Remanence measurements were done with a 2G cryogenic magnetometer in the shielded room of the Laboratoire des Sciences du Climat et de l'Environnement (LSCE). The original paleointensity method of Thellier and Thellier [1959] was employed throughout. The samples were heated twice (direct and reverse fields) from room temperature to usually over 500°C with at least 11 steps of amplitude from 10°C to 50°C depending on the samples and the temperature range. The paleointensity furnace at the LSCE has a large internal diameter allowing the simultaneous treatment of over 100 half samples. Heating of the samples lasted ~ 4 hours, and the samples were allowed to cool naturally overnight. At the beginning of each heating, air was evacuated from the furnace with a primary pump. Then argon was alternatively flushed in and pumped out $\sim 7\text{-}8$ times, up to $\sim 100\text{-}110^\circ\text{C}$. A gentle stream of Ar was then maintained during the entire experiment. In addition, following a suggestion by P. Johnson, a few grams of activated charcoal were introduced in the furnace. The charcoal acts as a buffer to avoid oxidation/reduction of magnetite. Under these conditions the groundmass of the samples shows insignificant changes in color up to the highest temperatures.

A field of $40\ \mu\text{T}$, close to the present field intensity in Hawaii, was applied along the z axis of the samples during both heating and cooling, as suggested by Levi [1975]. We checked for thermochemical alteration of the samples by redetermining the partial thermal remanent magnetization (PTRM) at a given low-temperature interval after previous heating at higher temperature. The automatic temperature control of the furnace allows any given temperature to be reproduced within $1\text{-}2^\circ\text{C}$. The PTRM checks could therefore be made very accurately, at least every two temperature steps and usually at every step for the highest temperatures.

4. Temporal Framework

The different age determinations which have been used here to reconstruct the changes of the geomagnetic field intensity are summarized in Table 1. A radiocarbon date of ~40 ka has been obtained on a humic ashy soil at a depth of 182 m [Beeson *et al.*, 1996]. Ar/Ar and K/Ar radiometric dating have been difficult in most cases because of the low yields of radiogenic $^{40}\text{Ar}^*$ (1×10^{-15} mol) at each temperature step, masked by 20 to 50 times more atmospheric argon, and because of the very low K contents due to the tholeiitic composition of the basalts. Nevertheless, nine age determinations have been obtained. Seven Ar/Ar dates ranging from (132 ± 32) to (391 ± 40) kyr were obtained for lava flows distributed down the total length of the core. Two intermediate K/Ar ages of (352 ± 105) and of (378 ± 109) kyr were also obtained for flow 147 (720 m) and flow 164 (798 m), respectively. The description of these results is given elsewhere [Sharp *et al.*, 1996].

We have used this time frame for the interpretation of the results. Following Holt *et al.* [1996], age interpolation was performed as three separate linear fits (0-182 m, 182-418 m, and 418-940 m) using the $^{40}\text{Ar}/^{39}\text{Ar}$ dates, the radiocarbon date at 182 m and the constraint that the top of the core is approximately of zero age. The extrusion rate for the 940-1053 m section was taken equal to that calculated for the 418-940 m section. Within this approximation the extrusion rate was one flow per 610 years in the 420-326 kyr interval, one flow per 5.6 kyr between 326 and 39 kyr, and one flow per 1.6 kyr during the last 39 kyr. As stressed by Holt *et al.* [1996], age interpolation is intended to provide a first-order approximation of geomagnetic changes as a function of age downcore. However, rates of extrusion could be highly variable on short timescales.

5. Results

5.1. Rock Magnetic Characteristics

The rock magnetic characteristics of the HSDP core flows have already been partially addressed by Garnier *et al.* [1996]. High field thermomagnetic analyses document a variety of sample behaviors. At one extreme are perfectly reversible, concave-down curves continuously decreasing to zero with

Curie temperature close to 580°C. At the other extreme are curves characterized by a regular decrease of the induced magnetization up to ~350°C, then a second decrease with $T_c \approx 550^\circ\text{C}$ and nonreversible behavior. Figure 1 gives representative examples of the thermomagnetic analyses. There is a continuous range of spectra between the two extreme cases described above. However, curves such as those illustrated in Figures 1a, 1b, and 1c represent the behavior observed in 85% of the cases, while the case in Figure 1d is only observed in 15% of the cases.

Magnetic hysteresis analyses document low values of H_c and H_{cr} and an S ratio higher than 0.9 along the entire length of the core. Combined with the thermomagnetic analyses, this identifies magnetite with variable amounts of Ti as the main magnetic mineral in a large majority of the samples.

5.2. Inclination Record

As mentioned in section 1, a record of the inclination obtained using alternating field demagnetization on several samples per flow has already been published [Holt *et al.*, 1996]. The thermally cleaned determinations of the inclination reported here were obtained from Thellier experiments, using the half vectorial sum of the magnetization vectors measured after heating in normal and reverse fields at each step of the thermal treatment. Because inclination values depend only on the demagnetization of the natural remanent magnetization (NRM), the inclination record obtained here is more detailed than the paleointensity record.

Examples of demagnetization diagrams obtained from these experiments are shown in Figure 2. Apart from an occasional small viscous component of magnetization easily removed at low temperatures, the demagnetization diagrams are highly linear. Inclinations for individual samples were determined by principal component, least squares analysis [Kirschvink, 1980]. In general, we obtained three determinations per flow (for a total of 524 reliable inclination determinations), with good within-flow consistency (>70% of the flows have a $\pm 1\sigma$ uncertainties of $< 5^\circ$). The record of the flow inclination means and their $\pm 1\sigma$ uncertainties obtained from the Thellier experiments is given in Figure 3 as a function of depth and interpolated age.

For the Mauna Loa sequence (Figure 4a) the inclination record obtained with thermal demagnetization is quite consistent with the inclination results of Holt *et al.* [1996] obtained with alternating field (af) cleaning. Both records document an episode of nearly zero inclination (feature A of Holt *et al.* [1996]) which has occurred at about 35-40 ka and has been tentatively associated with the Laschamp event [Holt *et al.*, 1996]. Another episode (feature B) is documented by Holt *et al.* [1996] by three flows showing negative inclinations around 130 kyr (~260 m). Unfortunately, no sample corresponding to these flows (number 39.5, 40, and 42; unit 41 is not a flow) was available for the paleointensity study, so no comparison could be made in this case.

For the Mauna Kea sequence (Figure 4b), the af and thermally cleaned records of the inclination are also very similar. The thermal record, however, in addition to the reverse inclination episode at 320 m (feature C), documents one additional episode of reverse inclination for flow 64 (Feature D, see Figure 4b). As discussed in section 2, careful rechecking has not revealed evidence for an inversion (or its contrary) of this core section or that it may be part of a flow separate from

Table 1. Radiometric Datings of Samples From Different Horizons of the HSDP core

Method	Unit	Depth, m	Age, kyr
<i>Mauna Loa</i>			
^{14}C	24	182	38.6 ± 0.9
Ar/Ar	43	266	132 ± 32
<i>Mauna Kea</i>			
Ar/Ar	49	300	199 ± 9
Ar/Ar	57	325	232 ± 4
Ar/Ar	58	334	241 ± 5
Ar/Ar	75	418	326 ± 23
K/Ar	147	720	352 ± 105
K/Ar	164	798	378 ± 109
Ar/Ar	196	940	400 ± 26
Ar/Ar	211	995	391 ± 40

From Beeson *et al.* [1993] and Sharp *et al.* [1996]. Linear extrusion rates have been calculated between the top of the core and unit 24, between units 24 and 75, and between unit 75 and 196.

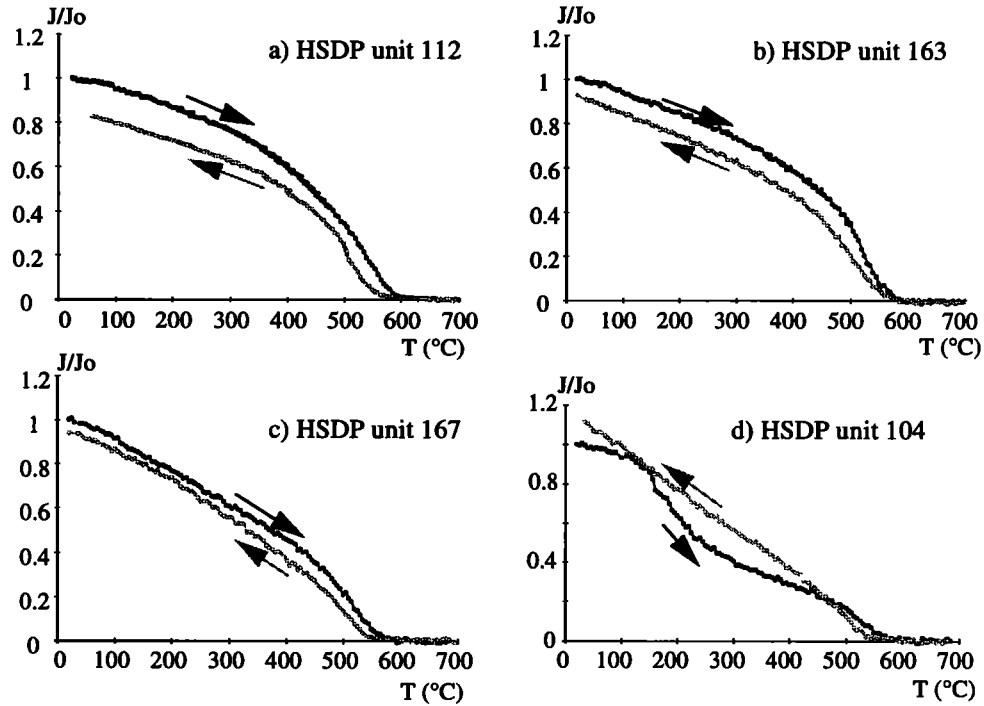


Figure 1. Representative thermomagnetic analyses plots obtained in an argon atmosphere. (a), (b), and (c) Typical behavior for low Ti-content magnetite obtained for ~85% of the samples. (d) Nonreversible behavior observed for ~15% of the samples, illustrating high-Ti content.

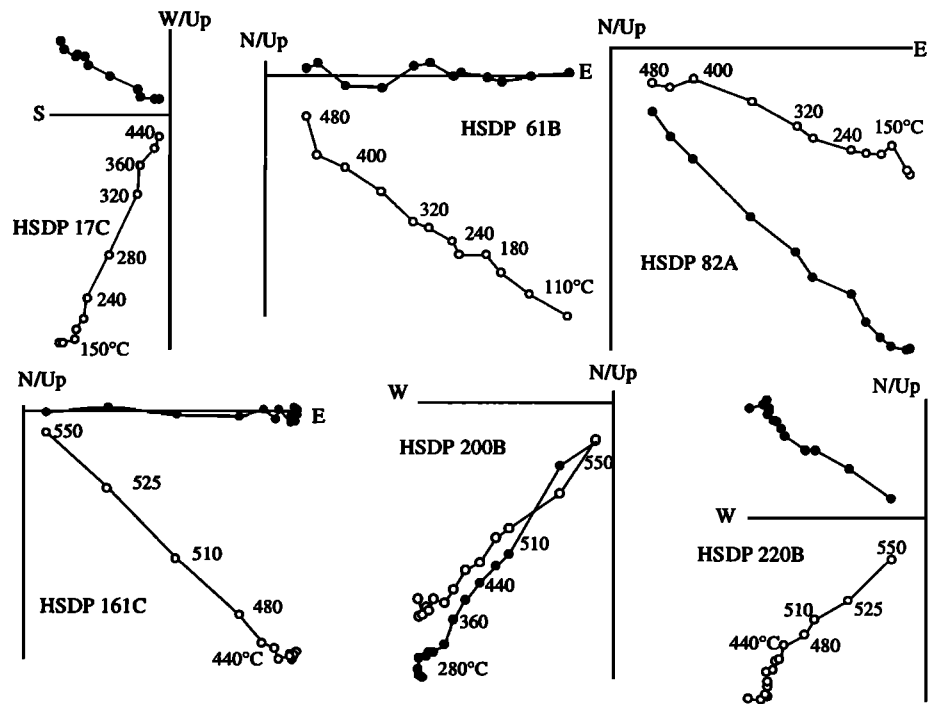


Figure 2. Typical demagnetization diagrams obtained using the half vectorial sum of the magnetization vectors measured after each double heating. Open and solid circles are projection onto the vertical and the horizontal planes, respectively. The core is not oriented in the horizontal plane so that the straight line passing through the solid dots has no directional meaning. Temperatures in $^{\circ}\text{C}$ are reported close to the corresponding points.

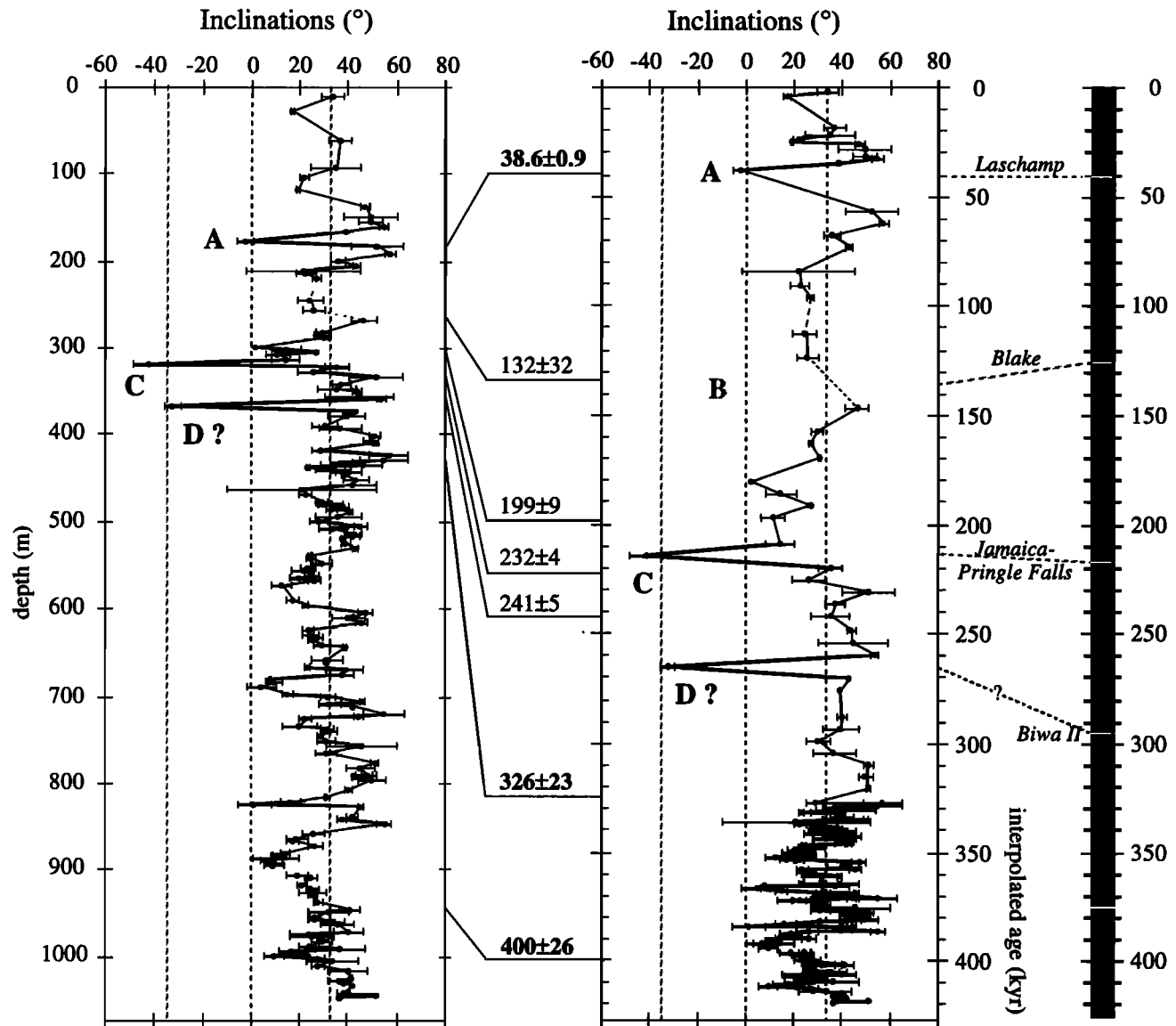


Figure 3. Inclination record obtained from HSDP core as a function of (left) depth and (right) interpolated ages. Radiometric datings are reported between the two diagrams and the ones in bold characters were used to calculate the interpolated timescale. An attempt has been made to correlate the inclination record to the geomagnetic timescale [Champion *et al.*, 1988; Opdyke and Channell, 1996]. Events A, B, and C are the same as those reported by Holt *et al.* [1996]. Event D is discussed in the text.

that used for the *af* inclination study. Therefore this inconsistency between the *af* and thermally cleaned records is not clearly understood. The observation that feature D is associated with a rather low paleointensity, also recorded by the overlying two flows, could corroborate the hypothesis of a real geomagnetic event. The interpolated age of feature D is 265 ka. The geomagnetic event which appears the closest in time to feature D is the Biwa II event, the age of which is 295 ka [Champion *et al.*, 1988]. Identification of feature D with this event would imply that either the section of the core used by Holt *et al.* [1996] was inverted or that the two sections belong to two separate flows.

As already described by Holt *et al.* [1996], the inclination record shows large, mostly continuous inclination swings ranging from ~ 0 to 65° . Short shifts of inclination away from these trends to shallow values are also present in the record.

Some of these shifts are followed by a continuation of the same trend of inclination as before the departure. This has led Holt *et al.* [1996] to suggest that these short-term events may not necessarily be related to the long-term variations.

5.3. Paleointensity Record

Representative examples of the paleointensity results are reported in Figure 5 as NRM/thermoremanent magnetization (TRM) (Arai) diagrams [Nagata *et al.*, 1963]. In these diagrams the residual natural remanent magnetization (NRM) is plotted versus the associated acquired thermoremanent magnetization (TRM). Both NRM and TRM values are normalized to the value of the NRM at room temperature. In an ideal diagram all the NRM/TRM points fall on a straight line, the slope of which gives the ratio between the applied laboratory field and the Earth's paleofield.

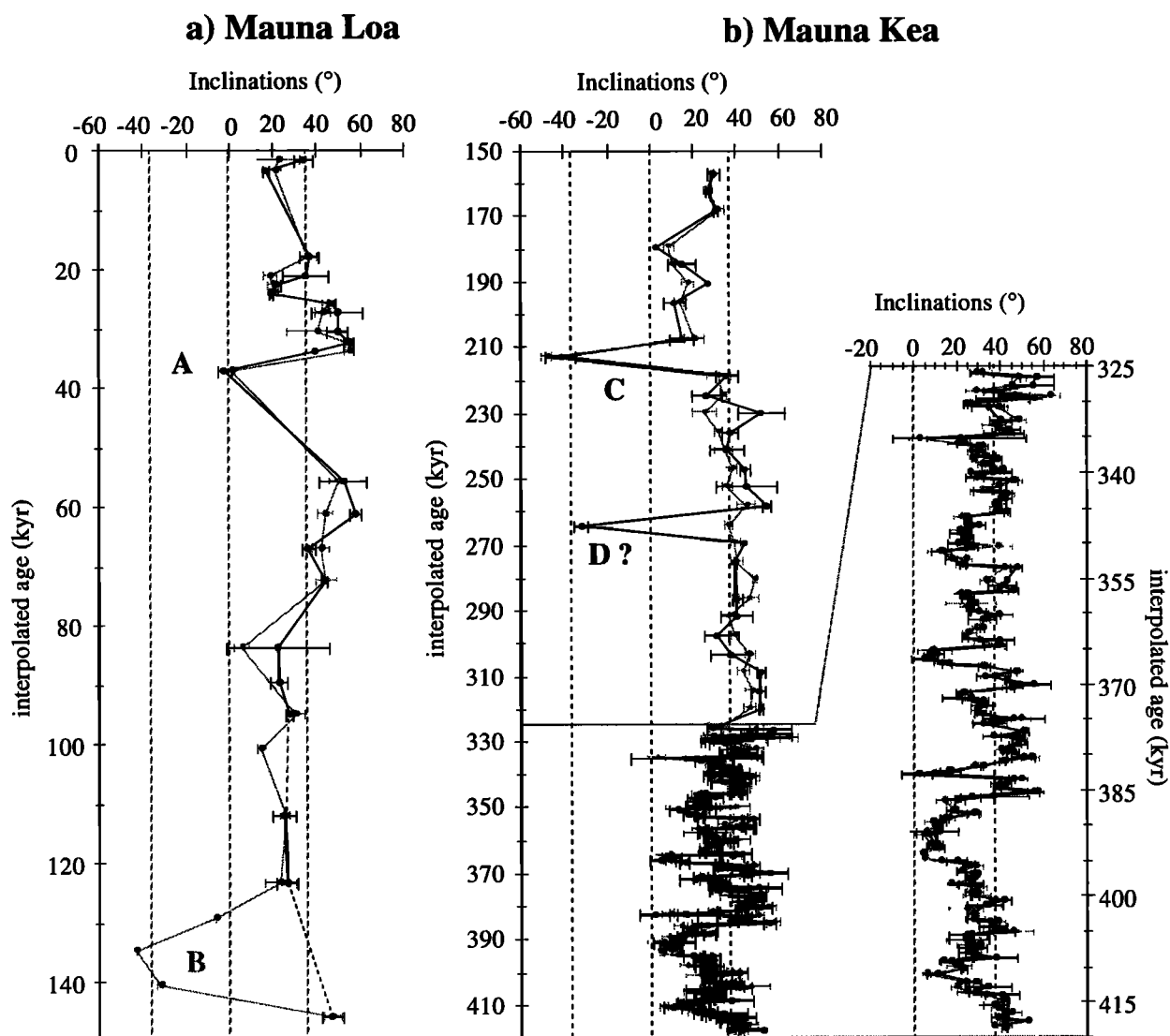


Figure 4. Comparison between the inclination data obtained using thermal treatment (solid dots, this study) and AF demagnetization (shaded dots, *Holt et al.* [1996]) for (a) the Mauna Loa sequence and (b) the Mauna Kea sequence. The bottom part of the Mauna Kea sequence has been enlarged.

As shown in Figure 5a, some of the diagrams from HSDP core are virtually ideal: a single straight line can be fitted precisely through the experimental points until almost complete removal of the initial NRM. These exceptionally accurate diagrams represent ~40% of the total. Although not quite as exceptional, many other diagrams meet published selection criteria and can reliably be interpreted in terms of geomagnetic field intensity, in spite of evidence of alteration during the laboratory heatings (Figure 5b).

The selection criteria used here are slightly more stringent than those commonly used in the literature. First, slopes defined by less than four points and corresponding to the removal of <20% of the total NRM ($f < 0.2$) were not used for paleointensity estimates (only three samples were accepted below this limit, while 92% of the accepted results have $f > 0.3$, 75% of them $f > 0.4$ and 52% $f > 0.5$). The diagrams were considered reliable up to the temperature at which magnetochemical transformations begin to occur, as

illustrated by nonlinearity in the NRM/TRM curve and negative PTRM checks. PTRM checks were considered negative when the new PTRM value at a given temperature differed from the previous one by >5% of the initial NRM. Only diagrams comprising at least three successful PTRM checks were considered reliable. No attempt was made to correct for negative PTRM checks using the correction recently proposed by *Valet et al.* [1996].

We checked carefully that the samples yielding linear Arai diagrams were also characterized by high directional stability (i.e., linear demagnetization plots tending to the origin), with no tendency for the magnetization to align along the laboratory field. This was easily done because the laboratory field was applied along the z axis of the samples ($I=0$) which was different from the direction of the magnetization for the overwhelming majority of the samples. Only for 13 samples did the magnetization move toward the laboratory field. Slope determinations were made using a least squares fitting of a

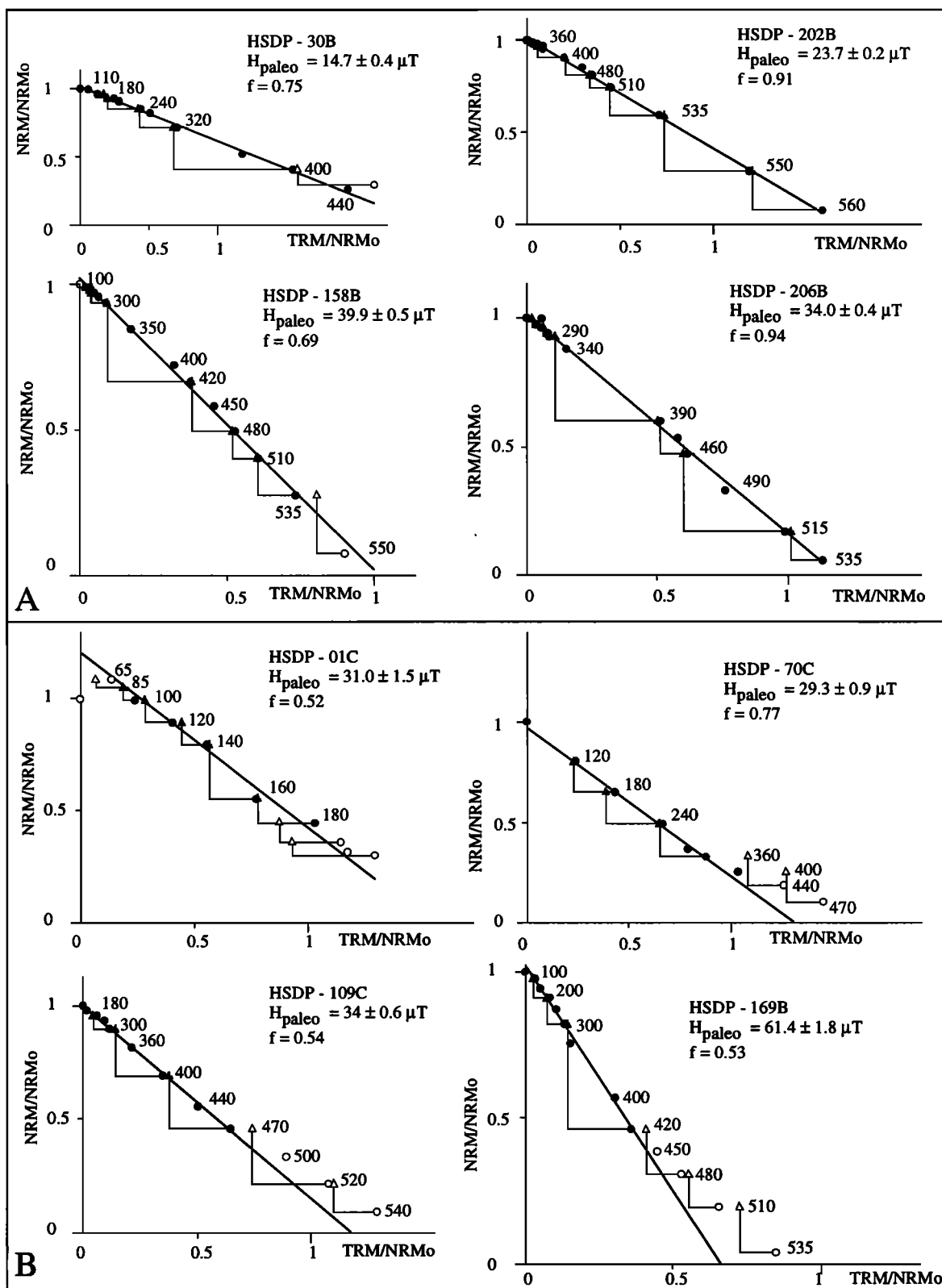


Figure 5. Representative NRM/TRM diagrams showing paleointensity estimates for HSDP core. Circles are NRM/TRM points calculated for each double heating at the temperature indicated close to the points. PTRM checks are reported with triangles. Solid (open) symbols correspond to the part of the diagram used (rejected) for the estimation of the paleointensity. (a) "Ideal" diagrams obtained for ~40% of the HSDP samples. (b) Other reliable diagrams obtained for ~38% of the samples.

straight line in the selected temperature interval. As a final rejection criterion, fits for which the correlation coefficient was <0.970 were considered unprecise and rejected.

Because a careful check has shown that some of the preliminary measurements reported by *Garnier et al.* [1996] may not be entirely reliable, we have systematically measured the half twin samples that had all been left untouched from this previous study. For 14 of the 105 samples we found significantly different results. In general, these samples correspond to the high paleointensities present in the *Garnier et al.* [1996] record, some of which are therefore not confirmed here. In addition, 21 samples which had been accepted in the preliminary study do not meet the stricter selection criteria used here. Finally, for the other 70 samples the paleointensity estimates obtained in the preliminary study are not significantly different from those obtained here. However, the associated precision parameters are almost systematically improved. This may be an effect of introducing the activated charcoal in the furnace, a technique that had not been used by *Garnier et al.* [1996]. For these reasons we do not use here any of the preliminary results, which should be considered entirely superseded by the ones reported here.

Table 2 reports all the successful paleointensity determinations with their associated precision parameters [*Coe et al.*, 1978]. The NRM fraction (f) is the percentage of the NRM taken into account for the determination; the gap factor (g) is a measure of how the NRM/TRM points are distributed along the straight-line segment, the more irregular the spacing between the selected points of the segment, the more (g) will decrease from unity. Finally, the factor q is a combination of these parameters ($q = bfg/s(b)$), where b is the slope of the straight line and $s(b)$ its standard error. Altogether, out of the 545 analyzed samples, we have obtained 425 reliable determinations from 174 flows. One flow is characterized by six determinations, 96 flows are characterized by three determinations, 54 are characterized flows by two determinations, and 23 flows are characterized by one determination. Only 16 flows did not yield any reliable estimate of the paleointensity.

The paleointensity record is shown in Figure 6, separately for the Mauna Loa (Figure 6a) and the Mauna Kea (Figure 6b) sequences, together with the associated inclination records. In a general way, the Mauna Loa sequence yielded somewhat disappointing results, both because some flows could not be sampled for the paleointensity study and because not all the samples yielded reliable results. Although not really detailed, the record does, however, document that the field strength was quite reduced in the period between 80 and 40 kyr and one determination indicates a very low paleointensity around 125 kyr. In the most recent period, between 30 and 20 kyr the field appears to have been close to its present value of about 40 μ T. There is then a huge gap so that nothing can be inferred for the 20 ka to present time interval.

The Mauna Kea sequence (Figure 6b) yields a much more detailed paleointensity record. In the upper period (326-132 kyr) the resolution is limited by the extrusion rate, but the record is sufficiently detailed to document that the geomagnetic field strength has undergone large oscillations with values from 15 to 60 μ T, over periods of 20-30 kyr. The lower part of the sequence, characterized by a much higher resolution, also documents a high variability of the field which has oscillated between 20 and 60 μ T. There is a period of very low intensity at the very bottom of the core (395-420

kyr) and some highs at 380 and 357-370 kyr. The intensity was on the average close to its present value in the interval 357-345 kyr and slightly lower around 330-326 kyr.

6. Discussion

6.1. Time Constraints

When dealing with volcanic records of geomagnetic field changes, it is difficult to correctly evaluate the temporal characteristics of the sequence of the lava flows. The sporadic nature of volcanic extrusion may result in bursts of flows that repeatedly sample the same geomagnetic field vector. If the results were analyzed as independent readings of the field, an incorrect description of the field characteristics would then be obtained. For this reason, methods have been developed for estimating whether significant serial correlation exists between successive flows [*Mankinen et al.*, 1985; *McElhinny et al.*, 1996; *Vandamme and Bruneton*, 1998].

For HSDP core, where only the intensity and inclination, but not the declination, are recovered, these methods cannot be used. Fortunately, however, some features of the record provide evidence that the flows were emplaced with some regularity. First, we notice that if linear approximation between dated flows is used, then the Laschamp and Jamaica events have an interpolated age quite consistent with the ages for these events reported in the literature. The Blake event has an interpolated age of 135 kyr, which is at the upper limit but within the uncertainties of the ages reported for this event, between 105 and 138 ka [*Worm*, 1997]. The only large discrepancy would concern the identification of the reverse polarity feature D with the Biwa II event, which would imply a difference of some 30 kyr between interpolated and real age. However, given the doubts about the very existence of the reversed polarity discussed above, one cannot really judge of the significance of this difference.

Second, we have calculated the time self-correlation function of both the intensity and the inclination records. The time self-correlation function $\phi(\tau)$ of any time dependent physical quantity $f(t)$ fluctuating around zero is defined as the normalized averaged value of $f(t)f(t+\tau)$, where $f(t+\tau)$ is $f(t)$ shifted by the time increment τ [see, e.g., *Landau and Lifchitz*, 1967]. By definition, $\phi(0) = 1$. The correlation function then decreases with increasing τ , reaching noise level for τ of the order of the time constant characteristic of the fluctuations of $f(t)$. Therefore, for the fluctuations in geomagnetic inclination and intensity about the value expected for a geocentric dipole and the mean values, respectively, the time self-correlation function should decrease to zero for values of τ of the order of the time constants associated to the nondipole and dipole terms. These are of the order of 400 to 2000 years, respectively, as obtained from the analysis of the historical field by *Hulot and Le Mouél* [1994].

For the calculation of the time correlation functions the 420-326 kyr and the 326-39 kyr intervals were considered separately, because of their different average extrusion rates. In both cases the self-correlation functions were calculated with τ progressively incremented by steps of one flow (which is the "natural" time increment of the record), corresponding to 610 years or 5600 years, respectively, when linear interpolation is used. The 39 ka to present interval was not analyzed because the HSDP paleointensity record is not detailed enough in this period. The 95% noise levels were

Table 2. Successful Paleointensity Determinations for HSDP core.

Flow	Depth, m	Age, kyr	Sample	f	g	q	Fets.d., μT	$\{I\} \pm 1\sigma$, deg	$\{\text{Fe}\} \pm 1\sigma$, μT	VADM $\pm 1\sigma$, 10^{22}Am^2
1	12.0	1.6	A	0.94	0.58	10.4	47.2 \pm 2.5	33.6 \pm 4.3	37.0 \pm 8.9	8.3 \pm 2.0
			B	0.54	0.78	8.0	32.7 \pm 1.8			
			C	0.52	0.79	8.4	31.0 \pm 1.5			
11	61.2	17.7	A	0.55	0.73	6.3	37.3 \pm 2.4	36.8 \pm 4.4	41.7 \pm 6.4	9.4 \pm 1.4
			B	0.50	0.84	13.4	49.0 \pm 1.6			
			C	0.68	0.86	23.7	38.8 \pm 1.0			
13	93.7	20.9	B	0.49	0.83	6.1	29.9 \pm 2.0	34.9 \pm 10.4	34.6 \pm 6.7	7.8 \pm 1.5
			C	0.36	0.80	5.4	39.4 \pm 2.1			
14	104.2	22.5	A	0.55	0.77	21.8	38.3 \pm 0.7	21.7 \pm 2.0	39.3 \pm 1.4	8.9 \pm 0.3
			B	0.59	0.76	23.5	40.9 \pm 0.8			
			C	0.63	0.86	36.2	38.7 \pm 0.6			
15	120.0	24.1	A	0.29	0.81	6.8	45.2 \pm 1.6	19.2 \pm 0.5	42.8 \pm 3.4	9.6 \pm 0.8
			B	0.49	0.86	14.7	40.4 \pm 1.2			
16	139.1	25.7	B	0.46	0.85	28.8	33.9 \pm 0.5	47.1 \pm 1.7	33.4 \pm 0.6	7.5 \pm 0.1
			C	0.66	0.90	38.6	33.0 \pm 0.5			
17	150.7	27.3	A	0.67	0.83	35.0	37.2 \pm 0.6	49.2 \pm 11.4	36.6 \pm 2.4	8.3 \pm 0.5
			B	0.78	0.85	22.2	34.0 \pm 1.0			
			C	0.83	0.82	44.6	38.7 \pm 0.6			
19	155.3	30.6	B	0.27	0.82	5.2	29.9 \pm 1.3	49.1 \pm 5.1	37.3 \pm 10.5	8.4 \pm 2.4
			C	0.34	0.73	4.8	44.7 \pm 2.3			
20	160.9	32.2	A	0.34	0.81	5.5	37.0 \pm 1.9	54.5 \pm 2.2	45.5 \pm 8.9	10.3 \pm 2.0
			B	0.32	0.86	5.2	54.8 \pm 3.0			
			C	0.34	0.88	6.3	44.7 \pm 2.2			
23	177.7	37.0	A	0.52	0.79	6.0	27.9 \pm 1.9	-2.3 \pm 3.3	29.4 \pm 2.1	6.6 \pm 0.5
			B	0.27	0.85	4.1	30.9 \pm 1.7			
27	184.5	55.5	B	0.68	0.74	6.1	17.0 \pm 1.4	51.9 \pm 10.8	15.3 \pm 2.4	3.5 \pm 0.5
			C	0.83	0.77	17.3	13.6 \pm 0.5			
28	191.4	61.1	A	0.57	0.76	16.4	16.4 \pm 0.4	57.2 \pm 2.5	19.9 \pm 3.1	4.5 \pm 0.7
			B	0.29	0.84	5.1	22.0 \pm 1.1			
			C	0.62	0.87	23.7	21.3 \pm 0.5			
29	199.7	66.8	A	0.53	0.80	14.6	12.9 \pm 0.4	35.9 \pm 3.1	15.0 \pm 1.9	3.4 \pm 0.4
			B	0.22	0.87	5.6	16.7 \pm 0.6			
			C	0.66	0.74	13.4	15.3 \pm 0.6			
30	205.1	72.4	A	0.52	0.83	17.0	14.2 \pm 0.4	43.1 \pm 1.5	14.0 \pm 1.0	3.2 \pm 0.2
			B	0.75	0.85	21.8	14.9 \pm 0.4			
			C	0.83	0.88	54.8	13.0 \pm 0.2			
33	214.0	89.3	B	0.43	0.69	10.5	17.5 \pm 0.5	22.5 \pm 4.0	15.3 \pm 3.2	3.4 \pm 0.7
			C	0.82	0.77	30.6	13.0 \pm 0.3			
34	221.2	95.0	C	0.74	0.87	34.1	34.4 \pm 0.7	26.9 \pm 1.9	34.5 \pm ---	7.8 \pm ---
39	256.8	123.1	B	0.29	0.74	3.0	11.0 \pm 0.8	25.7 \pm 4.6	9.8 \pm 1.6	2.2 \pm 0.4
			C	0.61	0.69	13.5	8.7 \pm 0.3			
43	269.2	145.7	A	0.50	0.81	10.0	33.0 \pm 1.4	46.4 \pm 5.1	33.9 \pm 1.5	7.6 \pm 0.3
			B	0.77	0.76	20.2	33.1 \pm 1.0			
			C	0.43	0.87	9.5	35.7 \pm 1.4			
45	281.6	156.9	B	0.44	0.75	6.3	56.1 \pm 3.0	29.8 \pm 2.9	50.8 \pm 7.4	11.5 \pm 1.7
			C	0.54	0.87	18.5	45.6 \pm 1.2			
46	284.4	162.6	A	0.48	0.80	6.5	41.6 \pm 2.5	27 \pm 0.8	36.7 \pm 4.2	8.3 \pm 0.9
			B	0.82	0.82	24.9	34.9 \pm 0.9			
			C	0.47	0.86	13.4	33.7 \pm 1.0			
47	288.4	168.2	B	0.93	0.86	25.5	26.8 \pm 0.8	30.9 \pm 0.9	31.2 \pm 6.2	7.0 \pm 1.4
			C	0.49	0.71	6.0	35.5 \pm 2.1			
50	303.9	185.1	A	0.22	0.78	3.0	38.4 \pm 2.3	14.5 \pm 6.4	33.9 \pm 15.2	7.6 \pm 3.4
			B	0.46	0.75	8.4	17.0 \pm 0.7			
			C	0.30	0.86	5.6	46.2 \pm 2.2			
51	306.3	190.8	C	0.67	0.85	18.9	15.7 \pm 0.5	27.0 \pm ---	15.7 \pm ----	3.5 \pm ----
54	315.3	207.7	C	0.56	0.76	8.7	20.5 \pm 1.0	14.4 \pm 5.8	20.5 \pm ----	4.6 \pm ----
57	327.2	224.6	B	0.79	0.77	21.6	67.4 \pm 1.9	26.1 \pm 7.0	70.2 \pm 4.0	15.8 \pm 0.9
			C	0.54	0.83	5.7	73.0 \pm 5.9			
58	334.0	230.2	A	0.49	0.86	7.3	43.6 \pm 2.5	51.4 \pm 10.8	37.1 \pm 9.2	8.4 \pm 2.1
			C	0.55	0.84	6.8	30.5 \pm 2.1			
59	343.2	235.8	A	0.55	0.83	7.6	44.8 \pm 2.7	37.1 \pm 3.7	50.0 \pm 10.3	11.3 \pm 2.3
			B	0.47	0.83	7.8	43.3 \pm 2.2			
			C	0.68	0.85	27.2	61.9 \pm 1.3			
60	346.6	241.5	A	0.29	0.75	6.4	34.6 \pm 1.2	35.7 \pm 7.9	40.9 \pm 7.2	9.2 \pm 1.6
			B	0.36	0.77	7.3	39.5 \pm 1.5			
			C	0.58	0.72	9.4	48.7 \pm 2.2			
61	349.9	247.1	A	0.44	0.75	3.6	38.7 \pm 3.6	43.9 \pm 2.1	36.9 \pm 2.5	8.3 \pm 0.6
			C	0.48	0.85	6.2	35.1 \pm 2.3			
62	355.4	252.7	C	0.47	0.87	10.2	26.3 \pm 1.1	44.7 \pm 14.1	26.3 \pm ---	5.9 \pm ---
64	368.7	264.0	B	1.04	0.81	18.6	-16.8 \pm 0.8	-32.1 \pm 3.2	16.6 \pm 0.3	3.7 \pm 0.1
			C	0.72	0.82	7.4	-16.4 \pm 1.3			
65	372.1	269.6	A	0.64	0.86	17.8	36.2 \pm 1.1	43.4 \pm ---	36.2 \pm ---	8.2 \pm ---
66	375.0	275.3	B	0.45	0.79	6.0	31.7 \pm 1.9	39.3 \pm 0.3	31.7 \pm ---	7.1 \pm ---

Table 2. (continued)

Flow	Depth, m	Age, kyr	Sample	<i>f</i>	<i>g</i>	<i>q</i>	Fets.d., μT	{I}±1σ, deg	{Fe}±1σ, μT	VADM±1σ, 10 ²² Am ²
68	377.1	286.6	B	0.34	0.88	6.9	42.0±1.8	40.1±2.2	41.2±1.0	9.3±0.2
			C	0.30	0.79	5.3	40.5±1.9			
69	380.2	292.2	A	0.40	0.77	7.0	29.4±1.3	39.8±7.7	34.3±4.4	7.7±1.0
			B	0.36	0.77	5.0	35.8±2.0			
			C	0.80	0.75	71.0	37.8±0.3			
70	389.0	297.8	B	0.28	0.58	1.3	28.0±3.5	30.5±5.3	28.6±1.0	6.4±0.2
			C	0.77	0.82	19.8	29.3±0.9			
71	394.1	303.5	A	0.38	0.80	6.6	42.0±2.0	36.9±8.8	42.4±3.3	9.6±0.7
			B	0.3	0.69	1.9	45.9±5.1			
			C	0.55	0.84	11.6	39.4±1.6			
72	402.5	309.1	A	0.83	0.81	20.5	54.1±1.8	51.2±2.0	46.9±6.3	10.6±1.4
			B	0.42	0.73	2.7	42.2±4.8			
			C	0.83	0.85	15.4	44.5±2.1			
73	407.1	314.7	A	0.44	0.86	9.4	30.5±1.2	49.7±3.0	29.7±2.8	6.7±0.6
			B	0.27	0.78	7.4	32.0±0.9			
			C	0.61	0.79	11.0	26.6±1.2			
74	409.9	320.4	A	0.44	0.86	13.2	35.5±1.0	51.4±0.9	33.0±3.5	7.4±0.7
			C	0.43	0.87	12.3	30.5±0.9			
75	418.4	326.0	A	0.64	0.85	12.7	19.5±0.8	29.1±3.7	21.5±4.2	4.8±0.9
			B	0.48	0.75	10.1	18.6±0.7			
			C	0.32	0.82	7.0	26.4±1.0			
76	423.2	326.6	A	0.49	0.77	7.0	44.3±2.4	56.8±8.0	28.8±13.5	6.5±3.0
			B	0.29	0.77	8.0	22.5±0.6			
			C	0.51	0.80	9.6	19.7±0.8			
78	429.5	327.8	A	0.43	0.82	8.7	44.1±1.8	54.9±10.0	39.9±5.9	9.0±1.3
			C	0.63	0.83	7.6	35.7±2.5			
79	432.0	328.4	A	0.54	0.73	6.8	23.5±1.4	37.2±4.5	25.8±2.6	5.8±0.6
			B	0.59	0.73	8.8	28.6±1.4			
			C	0.78	0.82	65.2	25.2±0.2			
80	434.6	329.1	B	0.40	0.81	3.9	33.3±2.8	46.5±7.6	32.9±0.5	7.4±0.1
			C	0.54	0.84	17.0	32.5±0.8			
			B	0.62	0.85	20.0	31.6±0.8			
81	436.9	329.7	C	0.67	0.84	8.8	43.2±2.8	41.5±12.4	37.4±8.3	8.4±1.9
			C	0.70	0.78	17.6	22.7±0.7			
82	439.5	330.3	C	0.25	0.74	3.8	32.7±1.6	23.7±1.1	22.7±---	5.1±---
83	441.3	330.9	A	0.49	0.84	10.3	42.1±1.7	34.2±7.1	37.4±6.6	8.4±1.5
			B	0.57	0.73	11.3	29.3±1.1			
86	444.9	332.7	C	0.87	0.84	15.2	23.2±1.1	40.3±5.4	26.3±4.3	5.9±1.0
			C	0.87	0.84	15.2	23.2±1.1			
87	447.6	333.3	B	0.51	0.79	11.1	42.4±1.6	38.3±0.6	38.5±5.5	8.7±1.2
			C	0.66	0.78	16.3	34.6±1.1			
88	451.8	334.0	A	0.60	0.78	7.2	29.5±1.9	43.5±5.6	30.8±1.9	6.9±0.4
			B	0.67	0.75	10.4	29.8±1.5			
			C	0.79	0.75	15.5	33.0±1.3			
89	458.5	334.6	B	0.34	0.83	4.5	26.9±1.7	42.0±9.5	27.5±0.8	6.2±0.2
			C	0.61	0.82	9.9	28.1±1.4			
90	464.7	335.2	A	0.28	0.74	8.1	22.5±0.6	21.2±30.8	23.4±1.2	5.3±0.3
			C	0.34	0.79	4.7	24.3±1.4			
91	470.7	335.8	A	0.23	0.79	3.0	65.0±4.0	22.7±2.7	57.8±8.5	13.0±1.9
			B	0.83	0.84	23.1	48.4±1.5			
			C	0.59	0.73	10.4	60.0±2.5			
92	476.6	336.4	B	0.57	0.84	17.7	52.1±1.4	29.5±2.5	57.5±7.7	13.0±1.7
			C	0.46	0.80	11.1	63.0±2.1			
93	479.4	337.0	A	0.53	0.79	16.6	51.0±1.3	30.3±3.2	48.0±4.2	10.8±0.9
			C	0.57	0.81	18.9	45.0±1.1			
94	481.2	337.6	A	0.69	0.81	24.8	39.1±0.9	33.1±4.7	38.9±3.0	8.8±0.7
			B	0.76	0.81	23.8	41.8±1.1			
			C	0.51	0.65	13.5	35.8±0.9			
95	484.3	338.2	A	0.9	0.82	62.0	35.6±0.4	38.1±2.5	34.3±1.6	7.7±0.4
			B	0.9	0.81	83.4	34.8±0.3			
			C	0.93	0.77	72.4	32.5±0.3			
96	486.4	338.8	A	0.48	0.81	12.6	42.3±1.3	33.6±2.4	40.8±1.5	9.2±0.3
			B	0.56	0.83	17.9	40.6±1.1			
			C	0.62	0.84	18.2	39.3±1.1			
97	490.4	339.5	C	0.54	0.87	15.2	42.5±1.3	41.0±0.9	42.5	9.6±---
98	494.2	340.1	B	0.51	0.84	20.8	54.2±1.1	36.1±9.7	58.0±5.3	13.1±1.2
			C	0.44	0.86	7.3	61.7±3.2			
99	500.5	340.7	A	0.51	0.74	14.2	34.7±0.9	28.3±4.0	31.8±3.2	7.2±0.7
			B	0.39	0.79	6.9	32.8±1.5			
			C	0.37	0.76	9.1	28.3±0.9			
100	505.9	341.3	A	0.25	0.73	3.9	43.0±2.0	45.3±3.0	43.0±---	9.70±---
101	507.2	341.9	A	0.69	0.66	14.0	25.9±0.9	39.4±---	26.0±---	5.85±---
102	508.5	342.5	A	0.60	0.67	6.9	62.9±3.7	33.9±5.8	62.9±---	14.2±---
103	514.1	343.1	A	0.74	0.71	11.8	50.0±2.2	42.8±3.1	49.4±0.7	11.1±0.1
			B	0.74	0.49	22.5	49.5±0.8			

Table 2. (continued)

Flow	Depth, m	Age, kyr	Sample	<i>f</i>	<i>g</i>	<i>q</i>	Fcts.d., μT	(I)±1σ, deg	(Fe)±1σ, μT	VADM±1σ, 10 ²² Am ²
104	516.9	343.7	C	0.80	0.55	10.8	48.6±2.0	42.0±3.1	45.0±5.4	10.1±1.2
			A	0.22	0.78	2.7	39.9±2.6			
			B	0.55	0.87	18.7	44.3±1.1			
105	520.0	344.3	C	0.33	0.81	4.5	50.7±3.1	38.1±0.9	52.7±3.7	11.9±0.8
			A	0.43	0.78	9.1	56.9±2.1			
			B	0.68	0.84	16.7	50.9±1.8			
106	526.4	345.0	C	0.42	0.72	12.5	50.1±1.2	39.3±1.7	59.0±0.05	13.3±0.0
			A	0.43	0.80	9.0	59.0±2.3			
			B	0.41	0.77	6.2	58.9±3.0			
107	532.1	345.6	A	0.50	0.75	9.8	46.1±1.8	43.0±1.3	42.6±3.6	9.6±0.8
			B	0.53	0.83	8.1	38.9±2.2			
			C	0.55	0.84	10.6	42.8±1.9			
108	538.9	346.2	A	0.40	0.79	4.6	42.4±3.0	24.5±0.9	39.4±3.0	8.9±0.7
			B	0.40	0.79	8.1	36.3±1.4			
			C	0.50	0.83	18.1	39.4±0.9			
109	542.9	346.8	A	0.75	0.81	34.8	45.7±0.8	24.9±2.2	38.1±6.6	8.6±1.5
			B	0.50	0.85	12.0	34.6±1.2			
			C	0.54	0.83	25.9	34.0±0.6			
110	549.7	347.4	A	0.52	0.71	9.5	39.4±1.5	29.4±4.3	45.5±5.4	10.3±1.2
			B	0.42	0.82	12.3	47.7±1.4			
			C	0.38	0.75	8.5	49.5±1.7			
111	555.2	348.0	A	0.84	0.86	35.0	45.7±1.0	23.6±2.9	41.9±3.4	9.5±0.8
			B	0.84	0.85	51.4	40.8±0.6			
			C	0.77	0.81	37.6	39.3±0.6			
112	556.8	348.6	A	0.67	0.78	48.1	46.1±0.5	21.6±4.7	41.8±7.7	9.4±1.7
			B	0.90	0.86	39.7	46.4±0.9			
			C	0.36	0.71	9.9	33.0±0.9			
113	561.4	349.2	A	0.46	0.69	5.6	40.4±2.3	25.2±2.8	35.1±4.6	7.9±1.0
			B	0.94	0.89	88.0	32.3±0.3			
			C	0.41	0.63	11.0	32.6±0.8			
114	566.1	349.9	A	0.37	0.79	7.1	40.6±1.7	20.2±4.4	42.2±1.9	9.5±0.4
			B	0.63	0.82	33.4	44.2±0.7			
			C	0.84	0.85	19.3	41.7±1.6			
115	567.8	350.5	A	0.28	0.84	13.5	17.2±0.3	26.6±2.7	21.8±5.7	4.9±1.3
			B	0.48	0.74	7.1	20.1±1.0			
			C	0.44	0.75	7.2	28.2±1.3			
116	574.7	351.1	A	0.31	0.67	8.5	34.1±0.8	12.8±4.4	34.3±0.1	7.7±0.0
			B	0.96	0.82	82.4	34.4±0.3			
			C	0.74	0.75	31.1	34.3±0.6			
118	590.6	352.3	A	0.26	0.79	2.6	48.8±3.9	17.3±2.8	44.8±3.9	10.1±0.9
			B	0.34	0.82	5.5	44.5±2.3			
			C	0.47	0.71	14.6	41.1±0.9			
119	597.2	352.9	B	0.77	0.78	19.7	20.7±0.6	22.6±1.4	19.8±1.3	4.5±0.3
			C	0.66	0.76	15.9	18.9±0.6			
			A	0.39	0.81	5.3	32.4±1.9			
120	604.7	353.5	B	0.75	0.86	21.4	37.8±1.1	47.2±3.1	36.0±3.1	8.1±0.7
			C	0.64	0.82	16.4	37.6±1.2			
			A	0.68	0.73	23.0	25.0±0.5			
123	609.9	355.4	B	0.68	0.73	23.0	25.0±0.5	42.3±0.7	27.6±3.6	6.2±0.8
			C	0.49	0.83	22.2	30.1±0.5			
			A	0.36	0.81	12.1	34.3±0.8			
124	610.5	356.0	B	0.52	0.79	15.7	42.5±1.1	40.4±6.6	37.6±4.3	8.5±1.0
			C	0.35	0.84	13.8	36.0±0.8			
			A	0.58	0.76	5.8	38.0±2.9			
125	616.1	356.6	B	0.46	0.73	8.0	39.0±1.6	45.8±2.1	37.2±2.2	8.4±0.5
			C	0.58	0.78	13.1	34.7±1.2			
			A	0.46	0.67	9.0	43.4±1.5			
126	625.8	357.2	B	0.76	0.87	17.5	33.8±1.3	23.9±2.4	39.6±5.1	8.9±1.1
			C	0.69	0.80	9.9	41.5±2.4			
			A	0.92	0.68	27.6	13.0±0.3			
127	629.4	357.8	C	0.41	0.88	11.6	38.1±1.2	24.9±3.1	25.6±17.7	5.8±4.0
			A	0.38	0.77	7.5	43.6±1.7			
			B	0.55	0.83	11.1	64.3±2.7			
128	632.7	358.4	C	0.51	0.84	12.9	76.0±2.6	27.5±2.2	61.3±16.4	13.8±3.7
			A	0.49	0.85	7.5	67.5±3.9			
			B	0.55	0.83	11.1	64.3±2.7			
129	636.2	359.0	A	0.49	0.85	7.5	67.5±3.9	25.6±1.8	67.5±---	15.2±---
			B	0.67	0.83	9.3	68.2±4.1			
			C	0.41	0.88	11.6	38.1±1.2			
130	642.7	359.6	A	0.32	0.78	5.3	49.3±2.3	29.4±3.5	68.2±---	15.4±---
			B	0.39	0.85	9.0	51.0±1.9			
			C	0.41	0.88	11.6	38.1±1.2			
131	645.5	360.2	A	0.32	0.78	5.3	49.3±2.3	39.0±0.8	50.2±1.2	11.3±0.3
			B	0.39	0.85	9.0	51.0±1.9			
			C	0.41	0.88	11.6	38.1±1.2			
132	657.8	360.9	A	0.56	0.85	10.3	46.0±2.1	31.6±6.7	35.8±8.8	8.1±2.0
			B	0.90	0.73	56.7	29.8±0.3			
			C	0.53	0.75	21.4	31.6±0.6			
134	662.0	362.1	A	0.37	0.82	7.3	40.5±1.7	31.6±0.6	43.1±2.3	9.7±0.5
			B	0.44	0.87	13.3	44.8±1.3			
			C	0.53	0.87	24.6	44.0±0.8			

Table 2. (continued)

Flow	Depth, m	Age, kyr	Sample	<i>f</i>	<i>g</i>	<i>q</i>	Fcts.d., μT	{I}±1σ, deg	{Fe}±1σ, μT	VADM±1σ, 10 ²² Am ²																																																																																																																																																																																																																																																																																																																																																																																																																																																																																																																																																																																		
136	666.0	363.3	A	0.47	0.75	8.2	64.2±2.8	23.4±1.2	65.6±1.9	14.8±0.4																																																																																																																																																																																																																																																																																																																																																																																																																																																																																																																																																																																		
			B	0.50	0.82	9.5	66.9±2.9				137	670.9	363.9	A	0.39	0.80	8.7	54.0±2.0	39.0±7.8	52.0±8.1	11.7±1.8	B	0.39	0.83	7.8	58.8±2.5	C	0.39	0.84	10.9	43.0±1.3	138	676.4	364.5	A	0.40	0.83	4.5	56.3±4.2	37.7±5.0	56.0±4.1	12.6±0.9	B	0.48	0.79	9.5	60.0±2.4	C	0.53	0.87	8.4	51.7±2.9	139	681.0	365.1	A	0.30	0.75	3.5	58.6±3.9	8.3±0.6	56.8±1.6	12.8±0.3	B	0.19	0.74	2.6	56.4±3.3	C	0.42	0.86	6.0	55.5±3.4	140	684.3	365.8	A	0.32	0.85	5.9	46.8±2.2	9.8±3.5	44.6±2.2	10.1±0.5	B	0.30	0.81	6.8	42.4±1.5	C	0.39	0.77	11.6	44.7±1.2	141	690.9	366.4	B	0.40	0.83	6.2	62.3±3.4	4.6±6.0	59.1±4.5	13.3±1.0	C	0.33	0.80	4.6	55.9±3.2	A	0.46	0.85	11.3	52.7±1.9	142	697.2	367.0	B	0.69	0.86	51.2	48.4±0.6	15.2±2.3	50.0±2.4	11.3±0.5	C	0.54	0.77	22.0	48.9±0.9	A	0.67	0.86	34.0	71.7±1.2	143	700.6	367.6	B	0.38	0.66	4.2	55.8±3.4	32.2±3.0	62.0±8.6	14.0±1.9	C	0.61	0.70	6.2	58.4±4.1	A	0.43	0.83	15.4	39.5±0.9	144	705.6	368.2	B	0.48	0.85	9.8	57.5±2.4	46.1±1.2	55.0±3.6	12.4±0.8	C	0.52	0.82	13.7	52.4±1.7	A	0.61	0.69	19.5	43.2±0.9	145	709.8	368.8	B	0.94	0.81	45.5	41.5±0.7	32.8±4.5	42.3±1.2	9.5±0.3	A	0.39	0.63	3.0	65.5±5.6	146	713.0	369.4	B	0.39	0.63	3.0	65.5±5.6	42.4±0.5	61.3±6.0	13.8±1.4	C	0.53	0.77	6.4	57.0±3.5	A	0.46	0.78	11.4	58.5±1.8	147	721.2	370.0	C	0.46	0.78	11.4	58.5±1.8	54.8±8.3	58.5±---	13.2±---	A	0.49	0.48	7.9	55.8±1.7	B	0.61	0.78	13.7	60.4±2.1	148	723.9	370.6	C	0.47	0.80	7.0	62.3±3.4	44.6±2.2	59.5±3.3	13.4±0.7	A	0.43	0.83	15.4	39.5±0.9	B	0.66	0.85	22.6	44.4±1.1	149	727.0	371.3	C	0.71	0.80	16.1	36.5±1.3	22.6±3.0	40.2±4.0	9.1±0.9	B	0.38	0.85	6.9	31.3±1.5	A	0.42	0.73	5.9	39.6±2.1	150	733.9	371.9	B	0.38	0.85	6.9	31.3±1.5	20.2±7.0	35.4±5.9	8.0±1.3	C	0.42	0.73	5.9	39.6±2.1	A	0.21	0.76	2.4	34.0±2.3	151	736.7	372.5	B	0.98	0.85	50.5	26.4±0.4	31.6±2.8	29.6±3.9	6.7±0.9	C	0.98	0.87	45.0	28.3±0.5	A	0.58	0.74	10.4	37.5±1.6	152	741.1	373.1	B	0.45	0.84	21.7	39.3±0.7	32.5±3.2	38.0±1.2	8.6±0.3	C	0.60	0.83	12.1	37.1±1.5	A	0.43	0.84	7.3	44.2±2.2	153	746.7	373.7	B	0.36	0.79	17.6	40.6±0.7	28.7±1.3	43.8±2.9	9.9±0.7	C	0.50	0.80	6.6	46.5±2.9	A	0.46	0.76	11.5	38.0±1.2	154	752.2	374.3	B	0.46	0.76	11.5	38.0±1.2	31.5±3.7	38.0±---	8.6±---	A	0.49	0.72	6.5	37.9±2.1	B	0.87	0.90	50.6	29.7±0.5	155	758.6	374.9	C	0.29	0.69	2.6	33.5±2.6	45.9±14.5	33.7±4.1	7.6±0.9	A	0.33	0.75	4.6	35.0±1.9	B	0.65	0.70	21.1	42.9±0.9	156	765.1	375.5	C	0.72	0.62	15.2	27.4±0.8	31.3±4.4	35.1±7.7	7.9±1.7	A	0.42	0.76	7.0	48.0±2.3	B	0.69	0.87	48.4	39.9±0.5	158	776.5	376.8	C	0.80	0.77	39.1	40.5±0.6	51.3±1.6	42.8±4.5	9.6±1.0	A	0.42	0.76	7.0	48.0±2.3	B	0.69	0.87	48.4	39.9±0.5	159	783.9	377.4	B	0.71	0.86	40.6	38.8±0.6	45.3±5.7	40.5±2.3	9.1±0.5	C	0.35	0.73	8.9	42.1±1.2	A	0.48	0.82	9.2	51.0±2.2	160	790.5	378.0	B	0.39	0.82	9.5	51.0±1.7	48.0±2.6	51.0±0.0	11.5±0.0	A	0.80	0.80	33.4	46.3±0.9	161	792.0	378.6	B	0.94	0.80	57.0	46.0±0.6	47.7±4.2	47.1±1.6	10.6±0.4	C	0.89	0.78	65.7	49.0±0.5	A	0.58	0.53	12.2	50.4±1.3	163	794.0	379.8	B	0.59	0.46	31.4	49.7±0.4	45.4±3.1	50.2±0.5	11.3±0.1	C	0.46	0.66	5.7	50.5±2.7	A	0.71	0.77	21.7	56.4±1.4	164	798.4	380.4	C	0.80	0.84	33.8	59.3±1.2	49.9±5.5	57.8±2.1	13.0±0.5	B	0.80	0.84	33.8	59.3±1.2	165	807.8	381.0	A	0.87	0.85	20.0	30.8±1.1	40.5±1.7	33.2±3.4	7.5±0.8	C	0.56	0.80	11.6	35.5±1.4	166	816.0	381.7	A	0.35	0.77	7.3	72.3±2.7	31.2±0.3	62.0±17.2	14.0±3.9	B	0.35	0.74	9.1
137	670.9	363.9	A	0.39	0.80	8.7	54.0±2.0	39.0±7.8	52.0±8.1	11.7±1.8																																																																																																																																																																																																																																																																																																																																																																																																																																																																																																																																																																																		
			B	0.39	0.83	7.8	58.8±2.5																																																																																																																																																																																																																																																																																																																																																																																																																																																																																																																																																																																					
			C	0.39	0.84	10.9	43.0±1.3																																																																																																																																																																																																																																																																																																																																																																																																																																																																																																																																																																																					
138	676.4	364.5	A	0.40	0.83	4.5	56.3±4.2	37.7±5.0	56.0±4.1	12.6±0.9																																																																																																																																																																																																																																																																																																																																																																																																																																																																																																																																																																																		
			B	0.48	0.79	9.5	60.0±2.4																																																																																																																																																																																																																																																																																																																																																																																																																																																																																																																																																																																					
			C	0.53	0.87	8.4	51.7±2.9																																																																																																																																																																																																																																																																																																																																																																																																																																																																																																																																																																																					
139	681.0	365.1	A	0.30	0.75	3.5	58.6±3.9	8.3±0.6	56.8±1.6	12.8±0.3																																																																																																																																																																																																																																																																																																																																																																																																																																																																																																																																																																																		
			B	0.19	0.74	2.6	56.4±3.3																																																																																																																																																																																																																																																																																																																																																																																																																																																																																																																																																																																					
			C	0.42	0.86	6.0	55.5±3.4																																																																																																																																																																																																																																																																																																																																																																																																																																																																																																																																																																																					
140	684.3	365.8	A	0.32	0.85	5.9	46.8±2.2	9.8±3.5	44.6±2.2	10.1±0.5																																																																																																																																																																																																																																																																																																																																																																																																																																																																																																																																																																																		
			B	0.30	0.81	6.8	42.4±1.5																																																																																																																																																																																																																																																																																																																																																																																																																																																																																																																																																																																					
			C	0.39	0.77	11.6	44.7±1.2																																																																																																																																																																																																																																																																																																																																																																																																																																																																																																																																																																																					
141	690.9	366.4	B	0.40	0.83	6.2	62.3±3.4	4.6±6.0	59.1±4.5	13.3±1.0																																																																																																																																																																																																																																																																																																																																																																																																																																																																																																																																																																																		
			C	0.33	0.80	4.6	55.9±3.2																																																																																																																																																																																																																																																																																																																																																																																																																																																																																																																																																																																					
			A	0.46	0.85	11.3	52.7±1.9																																																																																																																																																																																																																																																																																																																																																																																																																																																																																																																																																																																					
142	697.2	367.0	B	0.69	0.86	51.2	48.4±0.6	15.2±2.3	50.0±2.4	11.3±0.5																																																																																																																																																																																																																																																																																																																																																																																																																																																																																																																																																																																		
			C	0.54	0.77	22.0	48.9±0.9																																																																																																																																																																																																																																																																																																																																																																																																																																																																																																																																																																																					
			A	0.67	0.86	34.0	71.7±1.2																																																																																																																																																																																																																																																																																																																																																																																																																																																																																																																																																																																					
143	700.6	367.6	B	0.38	0.66	4.2	55.8±3.4	32.2±3.0	62.0±8.6	14.0±1.9																																																																																																																																																																																																																																																																																																																																																																																																																																																																																																																																																																																		
			C	0.61	0.70	6.2	58.4±4.1																																																																																																																																																																																																																																																																																																																																																																																																																																																																																																																																																																																					
			A	0.43	0.83	15.4	39.5±0.9																																																																																																																																																																																																																																																																																																																																																																																																																																																																																																																																																																																					
144	705.6	368.2	B	0.48	0.85	9.8	57.5±2.4	46.1±1.2	55.0±3.6	12.4±0.8																																																																																																																																																																																																																																																																																																																																																																																																																																																																																																																																																																																		
			C	0.52	0.82	13.7	52.4±1.7																																																																																																																																																																																																																																																																																																																																																																																																																																																																																																																																																																																					
			A	0.61	0.69	19.5	43.2±0.9																																																																																																																																																																																																																																																																																																																																																																																																																																																																																																																																																																																					
145	709.8	368.8	B	0.94	0.81	45.5	41.5±0.7	32.8±4.5	42.3±1.2	9.5±0.3																																																																																																																																																																																																																																																																																																																																																																																																																																																																																																																																																																																		
			A	0.39	0.63	3.0	65.5±5.6																																																																																																																																																																																																																																																																																																																																																																																																																																																																																																																																																																																					
146	713.0	369.4	B	0.39	0.63	3.0	65.5±5.6	42.4±0.5	61.3±6.0	13.8±1.4																																																																																																																																																																																																																																																																																																																																																																																																																																																																																																																																																																																		
			C	0.53	0.77	6.4	57.0±3.5																																																																																																																																																																																																																																																																																																																																																																																																																																																																																																																																																																																					
			A	0.46	0.78	11.4	58.5±1.8																																																																																																																																																																																																																																																																																																																																																																																																																																																																																																																																																																																					
147	721.2	370.0	C	0.46	0.78	11.4	58.5±1.8	54.8±8.3	58.5±---	13.2±---																																																																																																																																																																																																																																																																																																																																																																																																																																																																																																																																																																																		
			A	0.49	0.48	7.9	55.8±1.7																																																																																																																																																																																																																																																																																																																																																																																																																																																																																																																																																																																					
			B	0.61	0.78	13.7	60.4±2.1																																																																																																																																																																																																																																																																																																																																																																																																																																																																																																																																																																																					
148	723.9	370.6	C	0.47	0.80	7.0	62.3±3.4	44.6±2.2	59.5±3.3	13.4±0.7																																																																																																																																																																																																																																																																																																																																																																																																																																																																																																																																																																																		
			A	0.43	0.83	15.4	39.5±0.9																																																																																																																																																																																																																																																																																																																																																																																																																																																																																																																																																																																					
			B	0.66	0.85	22.6	44.4±1.1																																																																																																																																																																																																																																																																																																																																																																																																																																																																																																																																																																																					
149	727.0	371.3	C	0.71	0.80	16.1	36.5±1.3	22.6±3.0	40.2±4.0	9.1±0.9																																																																																																																																																																																																																																																																																																																																																																																																																																																																																																																																																																																		
			B	0.38	0.85	6.9	31.3±1.5																																																																																																																																																																																																																																																																																																																																																																																																																																																																																																																																																																																					
			A	0.42	0.73	5.9	39.6±2.1																																																																																																																																																																																																																																																																																																																																																																																																																																																																																																																																																																																					
150	733.9	371.9	B	0.38	0.85	6.9	31.3±1.5	20.2±7.0	35.4±5.9	8.0±1.3																																																																																																																																																																																																																																																																																																																																																																																																																																																																																																																																																																																		
			C	0.42	0.73	5.9	39.6±2.1																																																																																																																																																																																																																																																																																																																																																																																																																																																																																																																																																																																					
			A	0.21	0.76	2.4	34.0±2.3																																																																																																																																																																																																																																																																																																																																																																																																																																																																																																																																																																																					
151	736.7	372.5	B	0.98	0.85	50.5	26.4±0.4	31.6±2.8	29.6±3.9	6.7±0.9																																																																																																																																																																																																																																																																																																																																																																																																																																																																																																																																																																																		
			C	0.98	0.87	45.0	28.3±0.5																																																																																																																																																																																																																																																																																																																																																																																																																																																																																																																																																																																					
			A	0.58	0.74	10.4	37.5±1.6																																																																																																																																																																																																																																																																																																																																																																																																																																																																																																																																																																																					
152	741.1	373.1	B	0.45	0.84	21.7	39.3±0.7	32.5±3.2	38.0±1.2	8.6±0.3																																																																																																																																																																																																																																																																																																																																																																																																																																																																																																																																																																																		
			C	0.60	0.83	12.1	37.1±1.5																																																																																																																																																																																																																																																																																																																																																																																																																																																																																																																																																																																					
			A	0.43	0.84	7.3	44.2±2.2																																																																																																																																																																																																																																																																																																																																																																																																																																																																																																																																																																																					
153	746.7	373.7	B	0.36	0.79	17.6	40.6±0.7	28.7±1.3	43.8±2.9	9.9±0.7																																																																																																																																																																																																																																																																																																																																																																																																																																																																																																																																																																																		
			C	0.50	0.80	6.6	46.5±2.9																																																																																																																																																																																																																																																																																																																																																																																																																																																																																																																																																																																					
			A	0.46	0.76	11.5	38.0±1.2																																																																																																																																																																																																																																																																																																																																																																																																																																																																																																																																																																																					
154	752.2	374.3	B	0.46	0.76	11.5	38.0±1.2	31.5±3.7	38.0±---	8.6±---																																																																																																																																																																																																																																																																																																																																																																																																																																																																																																																																																																																		
			A	0.49	0.72	6.5	37.9±2.1																																																																																																																																																																																																																																																																																																																																																																																																																																																																																																																																																																																					
			B	0.87	0.90	50.6	29.7±0.5																																																																																																																																																																																																																																																																																																																																																																																																																																																																																																																																																																																					
155	758.6	374.9	C	0.29	0.69	2.6	33.5±2.6	45.9±14.5	33.7±4.1	7.6±0.9																																																																																																																																																																																																																																																																																																																																																																																																																																																																																																																																																																																		
			A	0.33	0.75	4.6	35.0±1.9																																																																																																																																																																																																																																																																																																																																																																																																																																																																																																																																																																																					
			B	0.65	0.70	21.1	42.9±0.9																																																																																																																																																																																																																																																																																																																																																																																																																																																																																																																																																																																					
156	765.1	375.5	C	0.72	0.62	15.2	27.4±0.8	31.3±4.4	35.1±7.7	7.9±1.7																																																																																																																																																																																																																																																																																																																																																																																																																																																																																																																																																																																		
			A	0.42	0.76	7.0	48.0±2.3																																																																																																																																																																																																																																																																																																																																																																																																																																																																																																																																																																																					
			B	0.69	0.87	48.4	39.9±0.5																																																																																																																																																																																																																																																																																																																																																																																																																																																																																																																																																																																					
158	776.5	376.8	C	0.80	0.77	39.1	40.5±0.6	51.3±1.6	42.8±4.5	9.6±1.0																																																																																																																																																																																																																																																																																																																																																																																																																																																																																																																																																																																		
			A	0.42	0.76	7.0	48.0±2.3																																																																																																																																																																																																																																																																																																																																																																																																																																																																																																																																																																																					
			B	0.69	0.87	48.4	39.9±0.5																																																																																																																																																																																																																																																																																																																																																																																																																																																																																																																																																																																					
159	783.9	377.4	B	0.71	0.86	40.6	38.8±0.6	45.3±5.7	40.5±2.3	9.1±0.5																																																																																																																																																																																																																																																																																																																																																																																																																																																																																																																																																																																		
			C	0.35	0.73	8.9	42.1±1.2																																																																																																																																																																																																																																																																																																																																																																																																																																																																																																																																																																																					
			A	0.48	0.82	9.2	51.0±2.2																																																																																																																																																																																																																																																																																																																																																																																																																																																																																																																																																																																					
160	790.5	378.0	B	0.39	0.82	9.5	51.0±1.7	48.0±2.6	51.0±0.0	11.5±0.0																																																																																																																																																																																																																																																																																																																																																																																																																																																																																																																																																																																		
			A	0.80	0.80	33.4	46.3±0.9																																																																																																																																																																																																																																																																																																																																																																																																																																																																																																																																																																																					
161	792.0	378.6	B	0.94	0.80	57.0	46.0±0.6	47.7±4.2	47.1±1.6	10.6±0.4																																																																																																																																																																																																																																																																																																																																																																																																																																																																																																																																																																																		
			C	0.89	0.78	65.7	49.0±0.5																																																																																																																																																																																																																																																																																																																																																																																																																																																																																																																																																																																					
			A	0.58	0.53	12.2	50.4±1.3																																																																																																																																																																																																																																																																																																																																																																																																																																																																																																																																																																																					
163	794.0	379.8	B	0.59	0.46	31.4	49.7±0.4	45.4±3.1	50.2±0.5	11.3±0.1																																																																																																																																																																																																																																																																																																																																																																																																																																																																																																																																																																																		
			C	0.46	0.66	5.7	50.5±2.7																																																																																																																																																																																																																																																																																																																																																																																																																																																																																																																																																																																					
			A	0.71	0.77	21.7	56.4±1.4																																																																																																																																																																																																																																																																																																																																																																																																																																																																																																																																																																																					
164	798.4	380.4	C	0.80	0.84	33.8	59.3±1.2	49.9±5.5	57.8±2.1	13.0±0.5																																																																																																																																																																																																																																																																																																																																																																																																																																																																																																																																																																																		
			B	0.80	0.84	33.8	59.3±1.2																																																																																																																																																																																																																																																																																																																																																																																																																																																																																																																																																																																					
165	807.8	381.0	A	0.87	0.85	20.0	30.8±1.1	40.5±1.7	33.2±3.4	7.5±0.8																																																																																																																																																																																																																																																																																																																																																																																																																																																																																																																																																																																		
			C	0.56	0.80	11.6	35.5±1.4																																																																																																																																																																																																																																																																																																																																																																																																																																																																																																																																																																																					
166	816.0	381.7	A	0.35	0.77	7.3	72.3±2.7	31.2±0.3	62.0±17.2	14.0±3.9																																																																																																																																																																																																																																																																																																																																																																																																																																																																																																																																																																																		
			B	0.35	0.74	9.1	71.6±2.1																																																																																																																																																																																																																																																																																																																																																																																																																																																																																																																																																																																					
			C	0.95	0.85	24.3	42.2±1.4																																																																																																																																																																																																																																																																																																																																																																																																																																																																																																																																																																																					

Table 2. (continued)

Flow	Depth, m	Age, kyr	Sample	<i>f</i>	<i>g</i>	<i>q</i>	Fets.d., μT	{I}±1σ, deg	{Fe}±1σ, μT	VADM±1σ, 10 ²² Am ²
167	822.2	382.3	A	0.34	0.74	4.4	60.1±3.5	16.5±4.5	57.9±1.9	13.1±0.4
			B	0.40	0.82	8.0	57.0±2.4			
			C	0.43	0.81	7.0	56.7±2.9			
168	825.7	382.9	B	0.68	0.83	36.5	43.0±0.7	1.5±7.0	38.0±7.1	8.6±1.6
			C	0.53	0.88	25.3	33.0±0.6			
169	829.8	383.5	A	0.34	0.69	5.3	64.2±3.0	45.2±1.2	62.9±1.4	14.2±0.3
			B	0.53	0.79	14.0	61.4±1.8			
			C	0.29	0.78	5.0	63.0±2.9			
170	838.8	384.1	A	0.39	0.77	4.8	87.0±5.6	41.9±2.3	71.4±16.2	16.1±3.6
			B	0.60	0.83	17.7	54.7±1.6			
			C	0.33	0.83	3.4	72.5±5.9			
171	841.7	384.7	C	0.81	0.71	35.0	29.5±0.5	37.9±2.0	29.5±---	6.6±---
172	847.9	385.3	A	0.30	0.67	3.2	38.3±2.5	55.0±2.8	40.9±3.5	9.2±0.8
			B	0.47	0.84	9.0	44.9±2.0			
			C	0.49	0.85	10.0	39.6±1.7			
173	859.7	385.9	B	0.43	0.84	7.2	38.1±1.9	26.1±4.8	36.2±2.8	8.2±0.6
			C	0.35	0.83	5.5	34.2±1.9			
174	866.2	386.5	A	0.65	0.85	10.8	33.3±1.7	19.0±4.4	37.3±4.9	8.4±1.1
			B	0.77	0.85	23.4	36.0±1.0			
			C	0.57	0.77	11.1	42.7±1.7			
176	868.5	387.8	A	0.33	0.73	3.0	38.7±3.2	17.4±2.9	42.5±4.0	9.6±0.9
			B	0.42	0.85	7.6	46.7±2.2			
			C	0.42	0.78	10.3	42.0±1.4			
177	874.1	388.4	A	0.26	0.77	4.4	52.2±2.4	26.7±2.9	46.2±5.7	10.4±1.3
			B	0.45	0.76	7.6	40.9±1.9			
			C	0.44	0.79	5.9	45.5±2.7			
178	881.5	389.0	A	0.57	0.55	12.6	39.4±1.0	13.9±2.0	39.2±0.4	8.8±0.1
			B	0.49	0.75	10.6	38.8±1.4			
			C	0.54	0.89	12.0	39.5±1.6			
179	885.3	389.6	A	0.63	0.84	13.4	57.8±2.3	11.5±2.9	46.5±9.8	10.5±2.2
			B	0.46	0.79	10.6	40.5±1.4			
			C	0.72	0.84	22.1	41.2±1.1			
180	886.3	390.2	A	0.34	0.71	3.6	39.3±2.6	11.0±1.5	33.1±5.5	7.4±1.2
			B	0.57	0.78	22.5	30.9±0.6			
			C	0.84	0.87	36.6	29.0±0.6			
181	887.8	390.8	A	0.44	0.83	16.0	33.1±0.8	10.5±9.5	34.2±2.3	7.7±0.5
			B	0.72	0.85	26.9	32.7±0.7			
			C	0.87	0.88	46.6	36.8±0.6			
182	890.7	391.4	A	0.18	0.75	3.5	31.0±1.3	6.7±2.8	32.0±0.9	7.2±0.2
			B	0.47	0.75	22.1	32.3±0.5			
			C	0.62	0.73	29.1	32.7±0.5			
184	895.0	392.7	A	0.18	0.78	4.5	34.1±1.1	9.6±3.4	35.3±3.9	8.0±0.9
			B	0.65	0.75	34.6	32.1±0.5			
			C	0.87	0.77	50.3	39.7±0.5			
185	896.8	393.3	A	0.44	0.48	5.3	43.7±1.7	9.4±4.1	39.2±3.9	8.8±0.9
			B	0.89	0.72	30.8	37.4±0.8			
			C	0.68	0.77	53.1	36.5±0.4			
188	906.7	395.1	A	0.64	0.86	32.7	45.7±0.8	19.2±4.8	41.7±7.5	9.4±1.7
			B	0.66	0.83	23.4	46.3±1.1			
			C	0.90	0.86	111.3	33.1±0.2			
189	911.0	395.7	A	0.55	0.63	12.0	30.0±0.9	24.8±2.7	30.7±0.8	6.9±0.2
			B	0.68	0.8	16.7	31.5±1.0			
			C	0.36	0.82	4.4	30.7±2.1			
190	919.2	396.3	A	0.38	0.72	4.5	60.2±3.7	21.2±2.0	42.5±17.0	9.6±3.8
			B	0.62	0.77	14.4	26.2±0.9			
			C	0.73	0.85	31.0	41.1±0.8			
191	924.9	396.9	A	0.87	0.89	53.2	37.7±0.5	26.9±1.4	35.3±3.4	8.0±0.8
			B	0.43	0.81	15.3	32.9±0.8			
192	925.69	397.6	A	0.31	0.84	8.0	29.0±1.0	23.9±1.1	25.3±7.4	5.7±1.7
			B	0.76	0.75	19.0	16.9±0.5			
			C	0.50	0.88	19.9	30.2±0.7			
193	926.5	398.2	A	0.59	0.84	23.0	32.6±0.7	25.7±5.5	32.7±1.4	7.4±0.3
			B	0.48	0.84	17.3	31.4±0.7			
			C	0.32	0.8	3.7	34.2±2.4			
195	929.5	399.4	B	0.38	0.87	6.4	50.1±2.6	25.4±1.9	44.8±7.6	10.1±1.7
			C	0.43	0.84	9.1	39.4±1.6			
196	939.3	400.0	A	0.25	0.69	3.1	25.5±1.5	27.8±2.0	26.4±1.2	5.9±0.3
			C	0.31	0.73	6.2	27.2±1.0			
197	946.2	400.6	C	0.49	0.84	8.1	31.8±1.7	40.8±4.0	31.9±---	7.2±---
198	949.9	401.2	A	0.45	0.70	14.0	22.0±0.5	32.3±8.4	25.6±3.3	5.8±0.7
			B	0.53	0.75	14.4	26.3±0.7			
			C	0.49	0.74	7.0	28.5±1.5			

Table 2. (continued)

Flow	Depth, m	Age, kyr	Sample	<i>f</i>	<i>g</i>	<i>q</i>	Fets.d., μT	{I}±1σ, deg	{Fe}±1σ, μT	VADM±1σ, 10 ²² Am ²
200	955.9	402.4	A	0.9	0.84	106.3	22.4±0.2	26.4±2.0	23.7±1.3	5.3±0.3
			B	0.71	0.83	29.0	23.4±0.5			
			C	0.62	0.88	31.7	26.2±0.4			
			D	0.30	0.77	5.2	22.9±1.0			
			E	0.91	0.88	82.3	23.9±0.2			
			F	0.91	0.87	44.7	23.3±0.4			
201	958.8	403.1	A	0.62	0.76	35.2	21.6±0.3	26.5±2.6	25.7±6.3	5.8±1.4
			B	0.87	0.81	32.0	33.0±0.7			
			C	0.91	0.82	70.5	22.3±0.2			
202	961.8	403.7	A	0.50	0.83	21.1	27.6±0.5	34.5±4.7	24.6±2.7	5.5±0.6
			B	0.91	0.81	94.5	23.7±0.2			
			C	0.87	0.82	92.8	22.4±0.2			
203	964.8	404.3	A	0.56	0.85	10.2	41.3±1.9	35.8±6.6	41.3±---	9.3±---
204	972.9	404.9	A	0.25	0.81	3.6	29.1±1.6	40.5±6.0	32.1±9.6	7.2±2.2
			B	0.66	0.81	13.9	24.3±0.9			
			C	0.40	0.83	8.1	42.9±1.8			
205	975.4	405.5	A	0.43	0.80	4.9	43.4±3.1	24.4±8.5	43.8±0.6	9.9±0.1
			C	0.50	0.81	6.8	44.2±2.7			
206	979.5	406.1	A	0.49	0.75	13.8	33.0±0.9	25.1±9.2	33.2±0.7	7.5±0.2
			B	0.94	0.83	62.6	34.0±0.4			
			C	0.87	0.85	47.2	32.5±0.5			
207	981.6	406.7	A	0.61	0.83	14.4	38.0±1.3	29.7±2.1	41.0±2.6	9.2±0.6
			B	0.62	0.81	26.1	43.1±0.8			
			C	0.41	0.79	14.1	41.9±1.0			
208	984.8	407.3	A	0.66	0.81	24.9	36.6±0.8	29.4±4.0	35.5±1.5	8.0±0.3
			B	0.59	0.71	27.4	33.8±0.5			
			C	0.69	0.82	25.7	36.2±0.8			
209	989.5	408.0	A	0.44	0.75	14.1	31.0±0.7	24.2±4.1	28.5±3.2	6.4±0.7
			B	0.58	0.83	14.6	24.9±0.8			
			C	0.54	0.89	18.5	29.7±0.8			
210	992.0	408.6	A	0.45	0.79	6.7	29.0±1.6	36.9±10.1	32.7±5.2	7.4±1.2
			C	0.47	0.78	6.6	36.3±2.0			
211	995.1	409.2	A	0.41	0.77	8.3	27.7±1.1	17.0±5.4	29.3±1.5	6.6±0.3
			B	0.54	0.84	21.5	30.6±0.6			
			C	0.48	0.73	8.9	29.6±1.2			
212	997.2	409.8	C	0.42	0.85	4.9	18.8±1.4	18.3±---	18.8±---	4.2±---
213	999.0	410.4	A	0.32	0.86	9.9	28.4±0.8	22.6±1.4	25.0±3.0	5.6±0.7
			B	0.28	0.83	14.3	23.9±0.4			
			C	0.60	0.81	18.0	22.7±0.6			
214	1000.5	411.0	A	0.24	0.72	4.2	28.8±1.2	9.8±4.1	30.2±3.4	6.8±0.8
			B	0.29	0.80	6.1	27.6±1.1			
			C	0.26	0.82	3.1	34.0±2.4			
216	1002.7	412.2	A	0.30	0.83	5.5	37.8±1.7	27.7±2.9	35.9±2.0	8.1±0.4
			B	0.47	0.82	20.6	33.8±0.6			
			C	0.35	0.86	5.0	36.1±2.2			
217	1006.5	412.8	A	0.81	0.75	49.6	18.9±0.2	33.6±10.9	18.9±0.9	4.3±0.2
			B	0.89	0.80	52.6	18.0±0.2			
			C	0.91	0.78	61.4	19.7±0.2			
218	1011.2	413.5	B	0.90	0.85	86.8	17.5±0.1	27.8±2.5	17.9±0.6	4.1±0.1
			C	0.87	0.83	43.7	18.3±0.3			
219	1019.4	414.1	B	0.53	0.75	19.9	25.9±0.5	40.0±7.9	25.9±---	5.8±---
220	1025.2	414.7	B	0.42	0.78	7.2	21.6±1.0	41.5±0.7	25.1±4.9	5.7±1.1
			C	0.68	0.82	21.3	28.5±0.8			
221	1029.7	415.3	B	0.34	0.59	3.6	22.3±1.2	36.5±4.8	22.4±0.1	5.1±0.0
			C	0.49	0.89	11.9	22.5±0.8			
222	1032.8	415.9	A	0.26	0.83	2.8	20.2±1.6	38.2±---	20.2±---	4.6±---
223	1035.8	416.5	A	0.24	0.77	4.9	26.2±1.0	42.0±---	26.2±---	5.9±---
224	1042.2	417.1	A	0.23	0.77	3.1	40.8±2.4	38.2±2.5	37.0±5.4	8.3±1.2
			C	0.41	0.78	9.8	33.1±1.1			
226	1049.9	418.3	A	0.40	0.87	14.5	16.5±0.4	36.6±---	16.5±---	3.7±---

Ages are the interpolated ages (see text); *f*, *g*, and *q* are the NRM fraction, gap factor, and quality factor respectively [Coe *et al.*, 1978]. Fe is the paleointensity estimate for an individual sample and s.d. is its standard deviation [Prevot *et al.*, 1985]. {I} and {Fe} are the unweighted average inclination and paleointensity, respectively, with standard deviations. VADM is the virtual axial dipole moment with the corresponding standard error. Mean flow inclination was derived from accepted demagnetization diagrams, including those of samples which did not yield reliable paleointensity estimates.

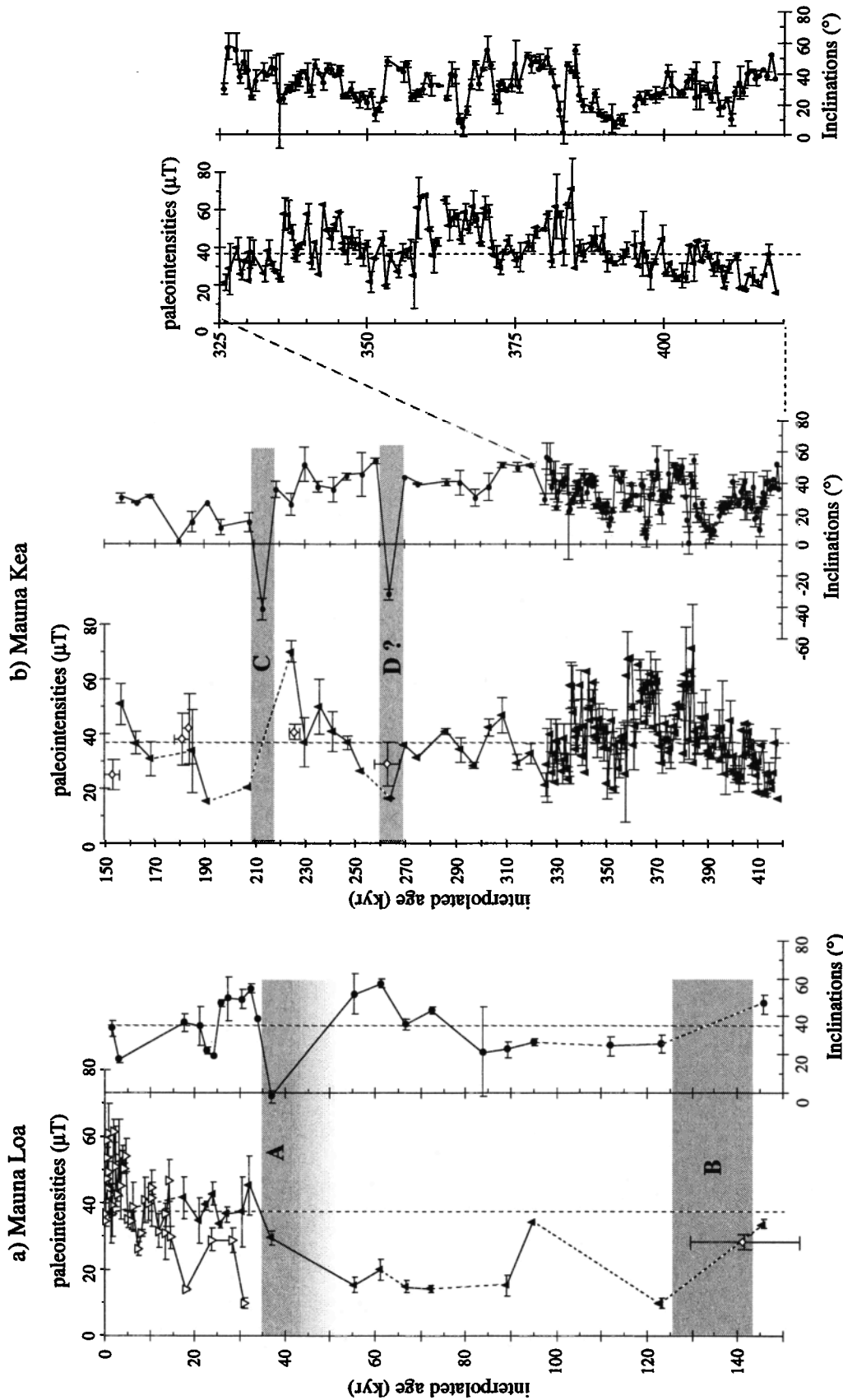


Figure 6. Paleointensity estimates for each unit of HSDP core (solid triangles) reported as a function of interpolated ages for (a) the Mauna Loa sequence and (b) the Mauna Kea sequence. The inclination records have also been reported for comparison (solid dots). The data are compared to the other data obtained also in Hawaii by open triangles from *Coe et al.* [1978], *Tanaka and Kono* [1991], and *Mankinen and Champion* [1993a, b] and open diamonds from *Brassart et al.* [1997]. Events A, B, C, and D discussed in the text are highlighted by shaded zones.

evaluated by generating a large number (>1000) of series made of uncorrelated random numbers, each series having a length equal to the number of data. The noise levels were taken equal to the limit not exceeded by 95% of the self-correlation functions calculated from these series.

In the 420-326 kyr interval (Figure 7a), the two correlation functions decrease to noise level for τ corresponding to a shift of two flows for the inclination record and of about four to five flows for the intensity. In the linear interpolation approximation this would correspond to ~1200 years for the inclination (i.e. halfway between estimates for the nondipole and dipole terms) and to ~2400-3000 years for the intensity (i.e., closely corresponding to a dipole term). In the 326-39 kyr interval, the intensity and inclination correlation functions both decrease sharply to below noise level after the first incremental step (Figure 7b), showing that in this interval, there is no correlation between successive flows, separated by an interpolated time interval of 5600 years. Although the self-correlation functions are not very sensitive to moderate changes in τ (i.e., rate of eruption), this

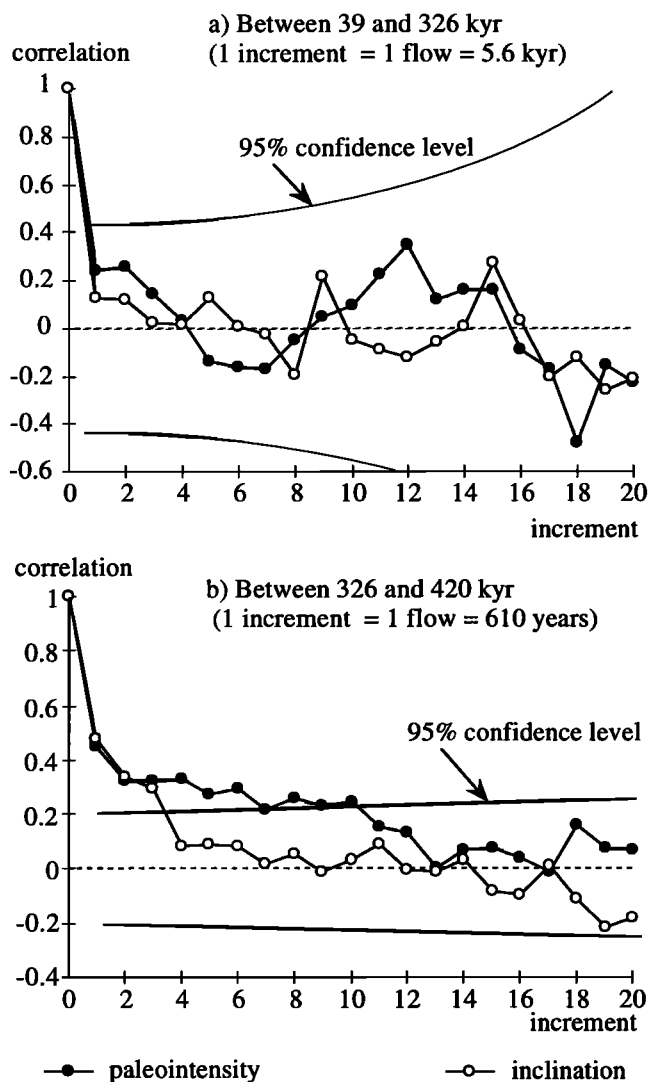


Figure 7. Self-correlation functions calculated for the paleointensity and the inclination records of core HSDP for two time intervals: (a) from 39 to 325 kyr; (b) between 326 and 420 kyr. See text for explanations and for the calculation of the 95% confidence level envelope.

Inclination anomalies ($^{\circ}$)

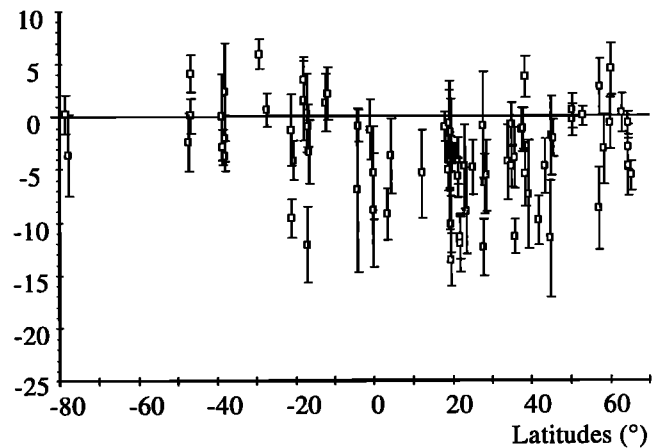


Figure 8. Inclination anomalies (difference between the observed inclination and the value expected for a geocentered dipole field) as a function of latitude. Open squares are data reported by *Johnson and Constable* [1997], solid square corresponds to the mean inclination calculated from the HSDP data set using the equations given by *McFadden and Reid* [1982].

coincidence between expected and observed values may be considered as an indication that the flows have been emplaced with some regularity.

In the discussion in sections 6.2 and 6.3, we have assumed a constant rate of extrusion (in flows per unit time) between the tie points. We are well aware that it is a first-order approximation, but it is the simplest approximation consistent with the available data.

6.2. Inclination Record and Short Events

The inclination record of the Mauna Loa sequence is very similar to that of *Holt et al.* [1996], although feature B is lacking because it has not been possible to drill additional samples for the paleointensity experiments in the very thin flows 42 and 40. The paleointensity estimate for flow 43 immediately below corresponds to the normal value at Hawaii, while that from flow 39 above feature B corresponds to a value of only 10 μT (Figure 6a). Thus it is reasonable to think that feature B corresponds to a rather low value of the geomagnetic field intensity, supporting the interpretation of this feature as a record of the Blake event [*Holt et al.*, 1996].

In the Mauna Kea sequence, feature C is observed in both the af-cleaned record of *Holt et al.* [1996] and that obtained from the Thellier experiments. It corresponds to a rather low paleointensity. The suggestion by *Holt et al.* [1996], based on age coincidence, that this feature is associated to the Jamaica/Biwal/Pringle Falls event is thus supported by the paleointensity results. Feature D is observed on the thermally cleaned record only, and it is associated to a pronounced low in the paleointensity record down to 15 μT (Figure 6b). Although, as reported in section 2, it is possible that a core section may have been inverted, the synchronism between low inclination and low intensity may suggest that it is a real geomagnetic feature. In this case, as mentioned in section 5.2, it may be associated with the Biwa II event.

The mean inclination for all flows except the reverse ones, calculated using the method of *McFadden and Reid* [1982] for

inclination-only data is 32.4° , and the associated dispersion is 12.2° , in agreement with *Holt et al.* [1996]. The mean value is smaller than the value of 35.6° expected from a geocentric dipole field but is consistent with data from sites in the same latitudinal band recently reported by *Johnson and Constable* [1997] (Figure 8).

The mean value is also consistent with the value of $30.4^\circ \pm 2.0^\circ$ obtained for synthetic sequences sampled at a constant rate of 600 or 5600 years depending on the time interval. These sequences have been generated using the *Constable and Parker* [1988] secular variation model, where we have used the variance and mean values of the Gauss coefficient given by *Johnson and Constable* [1997] and a simulation of their temporal variation as given by *Constable* [1990].

6.3. The Paleointensity Record

6.3.1. Comparison with other data from Hawaii. As mentioned in section 5.3, the paleointensity record obtained from the Mauna Loa sequence is very incomplete: only one reliable result was obtained for the last 20 kyr, and the time interval 125-20 ka is not very detailed. Therefore it is difficult to compare these new results to those previously obtained in Hawaii, most of which concern this recent period.

Comparison with the results of *Coe et al.* [1978], *Tanaka and Kono* [1991], and *Mankinen and Champion* [1993a, b] obtained from ^{14}C dated lavas from the Big Island is, however, possible in the limited interval 17-30 ka. The results from HSDP yield a value some 15% higher than the two highest determinations from these authors and do not document the very low values present at the two extremes of this interval in the ^{14}C dated record. No comparison is made here with the results obtained from Core SOH-4 by *Garnier et al.* [1996] because a careful check has shown that they are not entirely reliable.

The important time interval 0-50 ka is thus not precisely documented by the results obtained here. The new results from Core SOH-4, which will be completed soon, will fill the 0-20 ka gap and in a general way yield a more detailed record for the last 50 kyr.

The paleointensity record from the Mauna Kea sequence is, on the other hand, very detailed, given the high rate of success of the Thellier experiments, particularly in the 326-420 ka interval where the extrusion rate is high (Figure 6b). Although yielding somewhat lower field strength, the results of *Brassart et al.* [1997] from six different sites of the Kohala Mountain in the northern part of Big Island, also reported in Figure 6b, are consistent with the HSDP record within their uncertainties. However, because they were obtained from isolated outcrops, they fail to document one of the major characteristics of the geomagnetic field at Hawaii, namely, the high temporal variability. This stresses the importance of studying continuous volcanic sequences for the description of geomagnetic field changes in the past.

6.3.2. Comparison with data from other areas. Figure 9 shows a comparison of the virtual axial dipole moments (VADMs) from HSDP core with coeval data from geographic areas other than Hawaii published in the literature (references in Figure 9). For clarity, the HSDP results have been reported with no error bars.

In the 0-50 kyr interval, precise comparison of the results from HSDP with those from other regions is made difficult by the incompleteness of the Mauna Loa record. In general, the

HSDP record documents field strengths slightly higher than from outside Hawaii (Figure 9a), with the exception of the data of *Mejia et al.* [1996], from basaltic glasses from the East Pacific Rise, which document paleointensities $\sim 40\%$ higher. Given the high scatter of the worldwide results, it is difficult to obtain robust conclusions on the strength of the field at Hawaii with respect to other parts of the world.

In the 50-200 kyr interval (Figure 9b), VADMs from Hawaii are quite consistent with the Etna and Vulcano Island results [*Tric et al.*, 1994; *Laj et al.*, 1997] and with the results of *Mejia et al.* [1996], but over a factor of 2 smaller than the Reunion Island VADMs [*Chauvin et al.*, 1991; *Rais et al.*, 1996]. As discussed by *Laj et al.* [1997], La Réunion has been a region of anomalously high field strength in the 70-125 ka interval.

Comparison of the HSDP data with results for periods older than 200 kyr is hindered by the extreme paucity of published data from other geographical regions and the lack of reliable datings. The few results of *Schnepp* [1996] and *Borisova* [1986] appear, however, quite consistent with the HSDP data reported here (Figure 9c).

6.3.3. The 420-326 kyr interval. We have examined this time interval with special attention because the high extrusion rate combined with a very unusually high rate of success of the Thellier experiments yield a very detailed record of the field changes. The record documents a period of low field strength at the bottom of the core, progressively building up to present-day values at about 395-385 kyr (Figure 6b). Short-lived fluctuations are superimposed on this general trend. High field strength is then observed between 385 and 355 kyr with values reaching $60 \mu\text{T}$, followed by a progressive decrease to average values and two successive large oscillations. Inclination changes over this period do not appear to be correlated to the intensity changes. As remarked by *Holt et al.* [1996], the data show a pattern of inclination swings which result in a series of repeating shallow inclination values, with a periodicity of the order of 10-50 kyr.

Although, as discussed above, the time control of the record, based on linear interpolation, must be considered with caution, we have performed spectral analysis of both records using the Program Analyse *[Paillard et al., 1996]*. The results are shown in Figure 10. The inclination record does show significant power at 36, 8, 5, and 4 kyr, confirming the qualitative suggestion of *Holt et al.* [1996]. The paleointensity record, on the other hand, does not show particularly high power at these frequencies. Inaccuracies in time should affect the two records in the same way, so that, although the higher noise level in the paleointensity record may partly mask the weakest peaks, these differences in spectral power suggest that temporal changes in inclination and intensity are to a certain extent decorrelated. This is consistent with the results from the self-correlation analysis which have shown different correlation times for the intensity and the inclination.

It may be worth noting that the periodicities evidenced here are consistent with the results from a fluid dynamic experiment dealing with elliptical deformation [*Aldridge and Seyed Mahmoud*, 1998]. Extrapolated to the size of the Earth, these results would yield frequencies of the order of 15-20 kyr (K. Aldridge, personal communication, 1998). Our record may therefore provide evidence that this kind of deformation may influence the mechanisms driving the geodynamo. As the

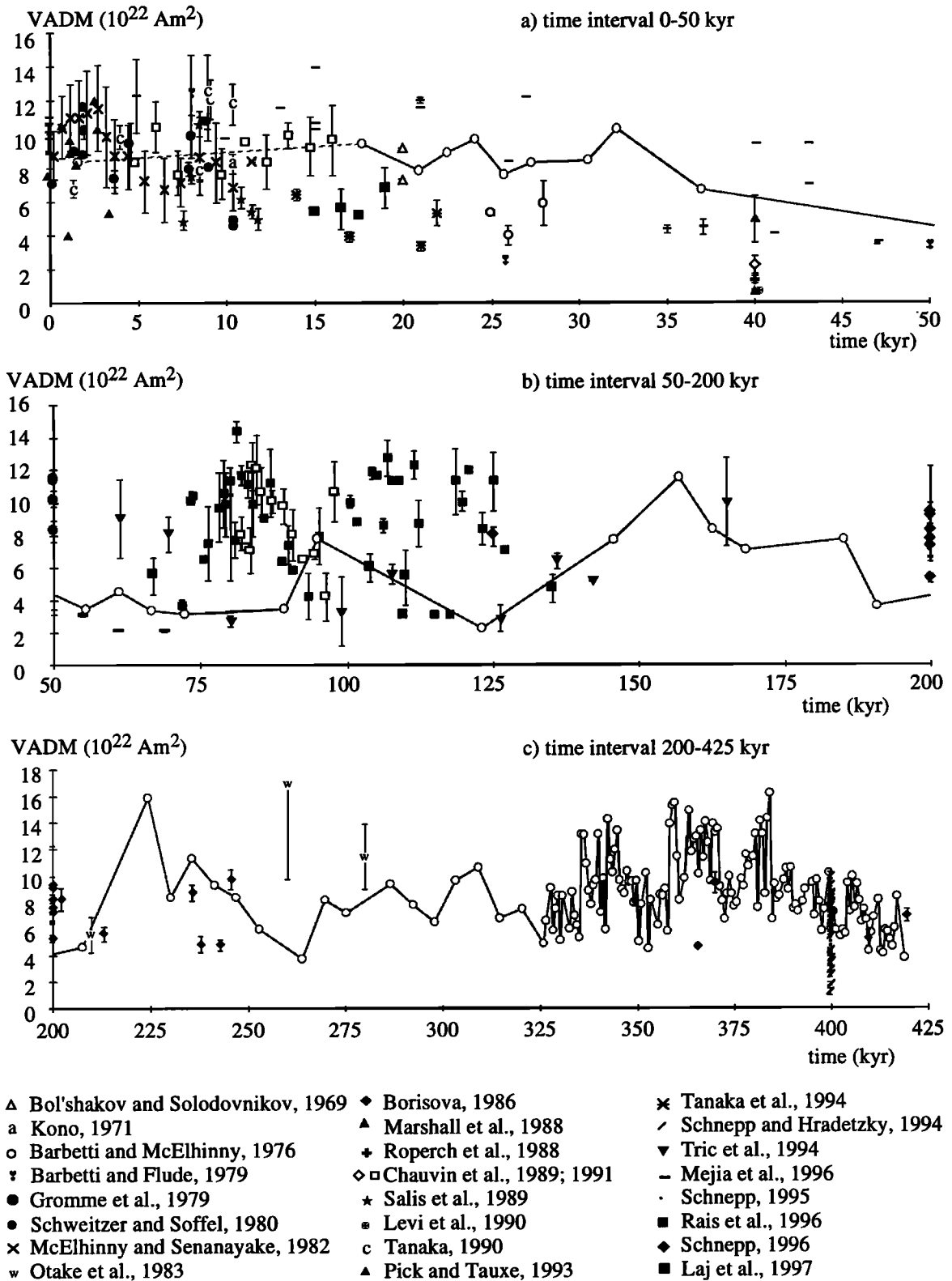


Figure 9. Virtual axial dipole moment as a function of time. Comparison between the HSDP record (shaded open dots linked by a line) and the volcanic data set obtained from other areas than Hawaii for different time intervals: (a) 0-50 kyr; (b) 50-200 kyr; and (c) 200-420 kyr.

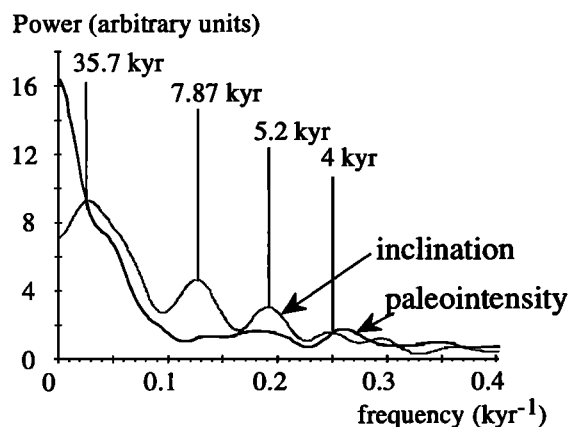


Figure 10. Spectral power analysis of the paleointensity and the inclination records from HSDP core for the time interval 325–420 kyr. No significant frequencies are visible on the paleointensity curve, while four periodicities exist in the inclination record.

HSDP is unique so far, we believe that further considerations on this issue will be possible only when additional data are available.

6.3.4. Statistical aspects. Given the large number of independent paleointensity determinations obtained here, we have also addressed the question of the statistical properties of the field. First, we have examined the histogram of the virtual dipole moments (VDMs) observed for the last 425 kyr. Figure 11 shows a comparison of this histogram with the distribution obtained by *Kono and Tanaka* [1995], which encompasses the last 2.5 Myr. Data from HSDP are more numerous than in the *Kono and Tanaka* [1995] 2.5 Myr database, but the two distributions have similar asymmetric shapes and yield very similar mean values for the VDM (8.3 ± 4.5 and $8.7 \pm 3 \times 10^{22}$ A.m²). Intensity variations from HSDP core appear to represent the entire variability of the field over 2.5 Myr.

We have also examined the distribution of the VADM from the HSDP core as a function of the deviation of the inclination from the value expected from a geocentered dipole field. The results are shown in Figure 12a, where the individual data have been grouped in bins to average out their intrinsic noise. As shown, only deviations up to 30° are considered because data beyond this value are not numerous enough for the average to be significant. Figure 12a clearly shows that there is no drastic decrease in intensity for deviations up to 30°, in sharp contrast with the findings of other authors [*Prévot et al.*, 1985; *Chauvin et al.*, 1990; *Mary and Courtillot*, 1993; *Lin et al.*, 1994; *Camps and Prévot*, 1996], which all suggest a relationship between changes in intensity and changes in direction (this holds true even taking into account that we only consider an inclination difference because no declination is available, whereas the other authors usually consider the distance between the VGP and the rotation axis). On the other hand, our results are consistent with the results of *Mankinen and Champion* [1993a, b]. Although less numerous and limited to the last 35 kyr, these last results do not document either any marked decrease of the intensity with the difference in inclination (Figure 12b). We think that this difference is due to the fact that while both *Mankinen and Champion* [1993a, b] and ourselves consider data encompassing a period during

which no reversal occurs, the results of *Prévot et al.* [1985], *Chauvin et al.* [1990], *Mary and Courtillot* [1993], *Lin et al.* [1994], and *Camps and Prévot* [1996] all consider data specifically from polarity transitions. The clear dependence of the intensity on the angular distance of the field from the rotation axis found by these authors may therefore be related to the reversal mechanisms rather than to the directional changes relative to secular variation. Unfortunately, no intermediate value of the inclination was recorded for any of the three excursions present in our record, so it proved impossible to examine whether the correlation intensity and angular distance did hold in these cases.

7. Conclusions

The HSDP record is the longest continuous volcanic record of geomagnetic field intensity yet reported. The inclination record, obtained from the half vectorial sum of thermally cleaned NRM, is quite consistent with the af-demagnetized results already reported by *Holt et al.* [1996]. The existence of an additional episode of negative inclination is suggested, but this episode could also result from an accidental inversion of a section of the core.

The average VDM ($8.7 \pm 3.0 \times 10^{22}$ A.m²), calculated from the HSDP data, is not significantly different from the value reported by *Kono and Tanaka* [1995] for the last 2.5 Myr, indicating that intensity variations observed from HSDP are representative for a longer period of time.

The unique continuity of the record allows description of the major temporal trends of the geomagnetic field at Hawaii with an as yet unattained accuracy. There are episodes of low and high field strength, from 15 to 60 μ T all along the explored time interval. Because these episodes are relatively short-lived, it is difficult to compare these results with published data from other parts of the world, which are not numerous and are usually obtained from isolated outcrops or short sequences. In a given short time interval, small

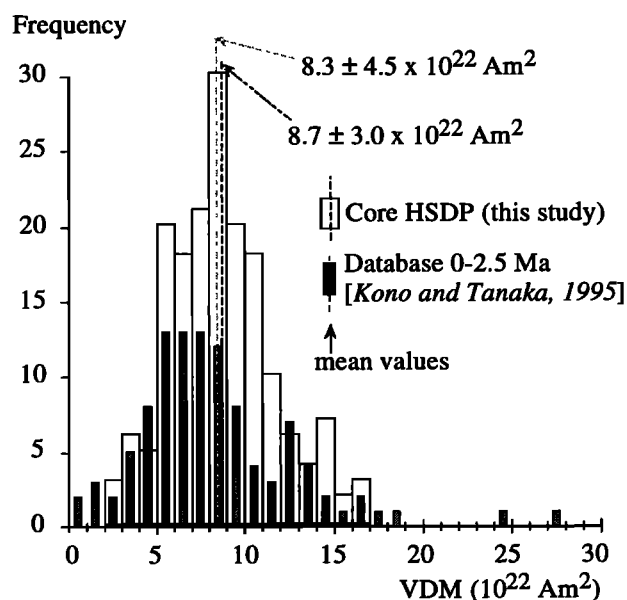


Figure 11. The distribution of VDMs from HSDP core compared to the distribution of nontransitional data over the last 0–2.5 Myr given by *Kono and Tanaka* [1995].

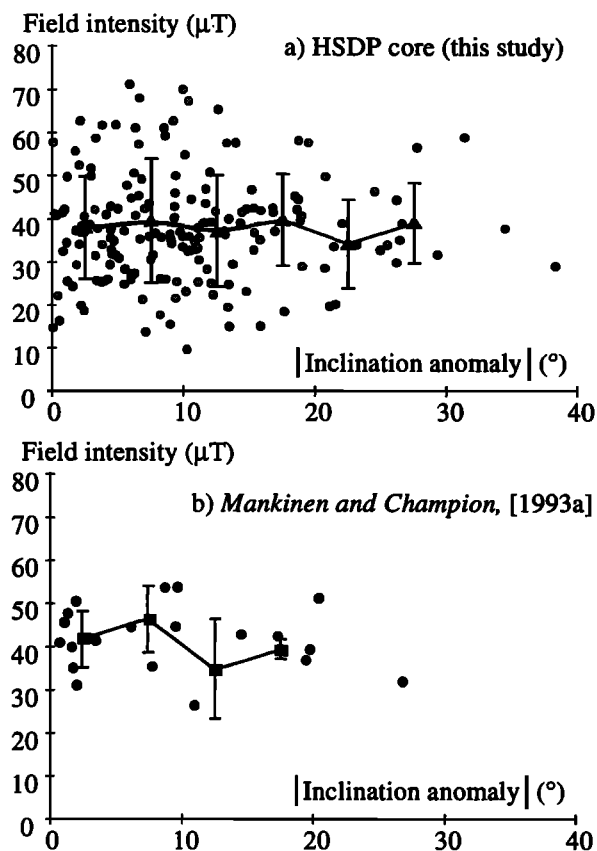


Figure 12. Field intensity as a function of inclination anomaly (in absolute value). A mean value has been calculated for each 5° interval in inclination. Individual data are reported as shaded dots and the mean values (a) as solid triangles for the HSDP data and (b) as solid squares for the data obtained by *Mankinen and Champion* [1993a], also from Hawaii.

inaccuracies in dating may therefore result in values higher, lower, or close to the oscillating HSDP record. It would therefore be hazardous to try to infer from these data precise information on the relative importance of the nondipole/dipole terms of the geomagnetic field at Hawaii during the explored time interval.

In the interval 420-326 kyr, the combination of high extrusion rate with an unusually high proportion of success of the Thellier experiments has yielded a very detailed record. Spectral analysis in this period shows that changes of the inclination and of the field strength may occur independently. The periodicities observed in the inclination spectrum are consistent with the results from a fluid dynamic experiment, dealing with elliptical deformation, extrapolated to the size of the Earth. If confirmed by future studies, this may indicate that this kind of deformation may have some impact on the mechanisms driving the geodynamo.

Although the geomagnetic events present in the inclination record are associated with low field strengths, the results do not document any marked decrease in intensity with deviations, up to 30°, of the inclination from the geocentric dipole value, in contrast with the findings of other authors but in agreement with the results of *Mankinen and Champion* [1993a, b]. We suggest that this difference is due to the fact that the HSDP record encompasses a period during which no

polarity transition, only short events occur, whereas the results showing a dependence of the intensity on the angular distance all consider data specifically from polarity transitions.

This study clearly shows that the analysis of long volcanic sequences yields valuable information on the temporal statistical characteristics of the geomagnetic field that cannot easily be obtained from the study of volcanic samples from isolated outcrops. Despite the time-consuming aspect of the measurements, this approach leads to a more accurate documentation of the field, especially when associated with high extrusion rates and high percentage of successful paleointensity determinations, two conditions which are well met by the HSDP core project.

Acknowledgements. We thank the three PIs of the HSDP project, Don DePaolo, Ed Stolper and Don Thomas, whose constant efforts have made the HSDP project possible, for allowing us to sample and for their constant encouragements. Ed Stolper is also thanked for providing the stratigraphy of the core in real-time during the sampling at Caltech. John Holt helped with the sampling and the numerous checks in the core repository. He and Joe Kirschvink are also warmly thanked for discussions. Emilio Herrero-Bervera participated to the sampling. Alain Mazaud and Nadia Szeremeta helped with the mathematical treatment. Finally, we warmly thank Scott Bogue, Hidefumi Tanaka, and the AE Michel Prévot for their most constructive reviews. Financial support was given by the CEA, the CNRS, and the CNRS-INSU DBT program Terre Profonde for the field trip. This is LSCE contribution 0221.

References

- Aldridge, K. D., and B. Seyed-Mahmoud, Spectral characteristics of elliptical instability in rotating ellipsoidal fluid shells: Applications to the Earth's fluid core, *Eos Trans. AGU*, 79 (17), Spring Meet. Suppl., S71, 1998.
- Barbetti, M., and M.W. McElhinny, The Lake Mungo geomagnetic excursion, *Philos. Trans. R. Soc. London, Ser.A*, 281, 515-542, 1976.
- Barbetti, M., and K. Flude, Geomagnetic variation during the Late Pleistocene period and changes in the radiocarbon time scale, *Nature*, 279, 202-205, 1979.
- Beeson, M. H., D. A. Clague, and J. P. Lockwood, Origin and depositional environment of clastic deposits in the Hilo drill hole, Hawaii, *J. Geophys. Res.*, 101, 11617-11629, 1996.
- Bol'shakov, A. S., and G. M. Solodovnikov, The field strength and the ancient field of the earth in the Pliocene-Quaternary epoch, *Izv. Earth Phys.*, 5, 325-328, 1969.
- Borisova, G.P., Estimation of the paleointensity of the geomagnetic field, *Izv. Acad. Sci. USSR Earth Phys. (Eng. Trans.)*, 22, 840-845, 1986.
- Brassart, J., E. Tric, J. P. Valet, and E. Herrero-Bervera, Absolute paleointensity between 60 and 400 ka from the Kohala Mountain (Hawaii), *Earth Planet. Sci. Lett.*, 148, 141-156, 1997.
- Camps, P., and M. Prévot, A statistical model of the fluctuations of the geomagnetic field from paleosecular variation to reversal, *Science*, 273, 776-779, 1996.
- Champion, D. E., M. A. Lanphere, and M. A. Kuntz, Evidence for a new geomagnetic reversal from lava flows in Idaho: Discussion of short polarity reversals in the Brunhes and the late Matuyama polarity chron, *J. Geophys. Res.*, 93, 11667-11680, 1988.
- Chauvin, A., R. A. Duncan, N. Bonhommet, and S. Levi, Paleointensity of the Earth's magnetic field and K-Ar dating of the Louchadière volcanic flow (central France): New evidence for the Laschamp excursion, *Geophys. Res. Lett.*, 16, 1189-1192, 1989.
- Chauvin, A., P. Roperch, and R. A. Duncan, Records of geomagnetic reversals from volcanic islands of French Polynesia, 2, Paleomagnetic study of a flow sequence (1.2-0.6 Ma) from the island of Tahiti and discussion of reversal models, *J. Geophys. Res.*, 95, 2727-2752, 1990.
- Chauvin, A., P. Y. Gillot, and N. Bonhommet, Paleointensity of the Earth's magnetic field recorded by two late Quaternary volcanic sequences at the island of La Réunion (Indian Ocean), *J. Geophys. Res.*, 96, 1981-2006, 1991.

- Coe, R. S., S. Grommé, and E. A. Mankinen, Geomagnetic paleointensities from radiocarbon-dated lava flows on Hawaii and the question of the Pacific nondipole low, *J. Geophys. Res.*, **83**, 1740-1756, 1978.
- Constable, C. G., A simple statistical model for geomagnetic reversals, *J. Geophys. Res.*, **95**, 4587-4596, 1990.
- Constable, C. G., and R. L. Parker, Statistics of the geomagnetic secular variation for the past 5 m.y., *J. Geophys. Res.*, **93**, 11569-11581, 1988.
- DePaolo, D. J., and E. M. Stolper, Models of Hawaiian volcano growth and plume structure: Implications of results from the Hawaii Scientific Drilling Project, *J. Geophys. Res.*, **101**, 11643-11654, 1996.
- Eiler, J. M., J. W. Valley, and E. M. Stolper, Oxygen isotope ratios in olivine from the Hawaii Scientific Drilling Project, *J. Geophys. Res.*, **101**, 11807-11813, 1996.
- Garnier, F., C. Laj, E. Herrero-Bervera, C. Kissel, and D. M. Thomas, Preliminary determinations of geomagnetic field intensity for the last 400 kyr from the Hawaii Scientific Drilling Project, Big Island, Hawaii, *J. Geophys. Res.*, **101**, 11665-11673, 1996.
- Grommé, S., E. A., Mankinen, M., Marshall, and R. S. Coe, Geomagnetic paleointensities by the Thelliers' method from submarine pillow basalts: Effects of seafloor weathering, *J. Geophys. Res.*, **84**, 3553-3575, 1979.
- Hauri, E. H., J. C. Lassiter, and D. J. DePaolo, Osmium isotope systematics of drilled lavas from Mauna Loa, Hawaii, *J. Geophys. Res.*, **101**, 11793-11806, 1996.
- Hawaii Scientific Drilling Project, *Core-Logs*, edited by E. Stolper and M. Baker, 471 pp., Calif. Inst. of Technol., Pasadena, 1994.
- Hofmann, A. W., and K. P. Jochum, Source characteristics derived from very incompatible trace elements in Mauna Loa and Mauna Kea basalts, Hawaii Scientific Drilling Project, *J. Geophys. Res.*, **101**, 11831-11839, 1996.
- Holt, J. W., J. L. Kirschvink, and F. Garnier, Geomagnetic field inclinations for the past 400 kyr from the 1-km core of the Hawaii Scientific Drilling Project, *J. Geophys. Res.*, **101**, 11655-11663, 1996.
- Hulot, G., and J. L. Le Mouél, A statistical approach to the Earth's main magnetic field, *Phys. Earth Planet. Inter.*, **82**, 167-183, 1994.
- Johnson, C. L., and C. G. Constable, The time average geomagnetic field: Global and regional biases for 0-5 Ma, *Geophys. J. Int.*, **131**, 643-666, 1997.
- King, J.W., and J.E.T. Channell, Sedimentary magnetism, environmental magnetism, and magnetostratigraphy, *U.S. Natl. Rep. Int. Union Geod. Geophys. 1987-1990*, *Rev. Geophys.*, **29**, 358-370, 1991.
- Kirschvink, J. L., The least square line and plane and the analysis of paleomagnetic data, *Geophys. J. R. Astron. Soc.*, **62**, 699-718, 1980.
- Kono, M. Intensity of the Earth's magnetic field in geological time, *J. Geomagn. Geoelectr.*, **23**, 1-9, 1971.
- Kono, M., and H. Tanaka, Intensity of the geomagnetic field in geological time: A statistical study, in: *The Earth's Central Part: Its Structure and Dynamics*, edited by T. Yukutake, pp75-94, Terra Sci., Tokyo, 1995.
- Laj, C., A. Raïs, J. Surmont, P. Y. Gillot, H. Guillou, C. Kissel, and E. Zanella, Changes of the geomagnetic field vector obtained from lava sequences on the island of Vulcano (Aeolian Islands, Sicily), *Phys. Earth Planet. Inter.*, **99**, 161-177, 1997.
- Landau, L., and E. Lifchitz, *Physique Statistique*, pp 583, MIR, Moscow, 1967.
- Lassiter, J. C., D. J. DePaolo, and M. Tatsumoto, Isotopic evolution of Mauna Kea volcano: First results from the 1-km drill core, *J. Geophys. Res.*, **101**, B5, 11769-11780, 1996.
- Levi, S., Comparison of two methods of performing the Thellier experiment (or, how the Thellier method should not be done), *J. Geomagn. Geoelectr.*, **27**, 245-255, 1975.
- Levi, S., S. H. Audunsson, R. A. Duncan, L. Kristjansson, P. Y. Gillot, and S. P. Jacobsson, Late Pleistocene geomagnetic excursion in Icelandic lavas: Confirmation of the Laschamp excursion, *Earth Planet. Sci. Lett.*, **96**, 443-457, 1990.
- Lin, J. L., K. L. Verosub, and A. P. Roberts, Decay of the virtual dipole moment during polarity transitions and geomagnetic excursions, *Geophys. Res. Lett.*, **21**, 525-528, 1994.
- Mankinen, E. A., and D. E. Champion, Broad trends in geomagnetic paleointensity on Hawaii during Holocene time, *J. Geophys. Res.*, **98**, 7959-7976, 1993a.
- Mankinen, E. A., and D. E. Champion, Latest Pleistocene and Holocene geomagnetic paleointensity on Hawaii, *Science*, **262**, 412-416, 1993b.
- Mankinen, E. A., M. Prévot, C. S. Grommé and R. S. Coe, The Steens Mountain (Oregon) geomagnetic polarity transition, 1, Directional history, duration of episodes, and rock magnetism, *J. Geophys. Res.*, **90**, 10393-10416, 1985.
- Marshall, M., A. Chauvin, and N. Bonhommet, Preliminary paleointensity measurements and detailed magnetic analyses of basalts from the Skalamaelifell excursion, southwest Iceland, *J. Geophys. Res.*, **93**, 11681-11698, 1988.
- Mary, C., and V. Courtillot, A three-dimensional representation of geomagnetic reversal records, *J. Geophys. Res.*, **98**, 22461-22475, 1993.
- McElhinny, M. W., and W. E. Senanayake, Variations in the geomagnetic dipole 1: The past 50 000 years, *J. Geomagn. Geoelectr.*, **34**, 39-51, 1982.
- McElhinny, M. W., P. L. McFadden, and R. T. Merrill, The myth of the Pacific dipole window, *Earth Planet. Sci. Lett.*, **143**, 13-22, 1996.
- McFadden P. L., and A. B. Reid, Analysis of palaeomagnetic inclination data, *Geophys. J. R. Astr. Soc.*, **69**, 307-319, 1982.
- Mejia, V., N. D., Opydyke, and M. R., Perfit, Paleomagnetic field intensity recorded in submarine basaltic glass from the East Pacific Rise, the last 69 ka, *Geophys. Res. Lett.*, **23**, 475-478, 1996.
- Moore, J. G., Subsidence of the Hawaiian ridge, *U.S. Geol. Survey Prof. Pap.*, **1350**, 85-100, 1987.
- Moore, J. G., B. L. Ingram, K. R. Ludwig, and D. A. Clague, Coral ages and island subsidence, Hilo drill hole, *J. Geophys. Res.*, **101**, 11599-11605, 1996.
- Nagata, T., Y. Arai, and K. Momose, Secular variation of the geomagnetic total force during the last 5000 years, *J. Geophys. Res.*, **68**, 5277-5282, 1963.
- Opydyke, N. D., and J. E. T. Channell, *Magnetic Stratigraphy*, Academic, San Diego, Calif., 1996.
- Otake, H., H. Tanaka, M. Kono, and K. Saito, Paleomagnetic study of Pleistocene lavas and dykes of the Zao volcano group, Japan, *J. Geomagn. Geoelectr.*, **45**, 595-612, 1983.
- Paillard, D., L. Labeyrie, and P. Yiou, Macintosh program performs time-series analysis, *Eos Trans. AGU*, **77**, 379, 1996.
- Pick, T., and L. Tauxe, Holocene paleointensities: Thellier experiments on submarine basaltic glass from the East Pacific Rise, *J. Geophys. Res.*, **98**, 17949-17964, 1993.
- Prévot, M., E. A. Mankinen, R. S. Coe, and C. S. Grommé, The Steens Mountain (Oregon) geomagnetic polarity transition, 2, Field intensity variations and discussion of reversal models, *J. Geophys. Res.*, **90**, 10417-10448, 1985.
- Raïs, A., C. Laj, J. Surmont, P. Y. Gillot, and H. Guillou, Geomagnetic field intensity between 70 000 and 130 000 years B.P. from a volcanic sequence on La Réunion, Indian Ocean, *Earth Planet. Sci. Lett.*, **140**, 173-189, 1996.
- Rhodes, J. M., Geochemical stratigraphy of lava flows sampled by the Hawaii Scientific Drilling Project, *J. Geophys. Res.*, **101**, 11729-11746, 1996.
- Roperch, P., N. Bonhommet, and S. Levi, Paleointensity of the Earth's magnetic field during the Laschamp excursion and its geomagnetic implications, *Earth Planet. Sci. Lett.*, **88**, 209-219, 1988.
- Salis, J.S., N. Bonhommet, and S. Levi, Paleointensity of the geomagnetic field from dated lavas of the Chaîne des Puys, France, 1.7-12 thousand years before present, *J. Geophys. Res.*, **94**, 15771-15784, 1989.
- Schnepp, E., Paleointensity study of Quaternary East Eifel phonolitic rocks (Germany), *Geophys. J. Int.*, **121**, 627-633, 1995.
- Schnepp, E., Geomagnetic paleointensities derived from volcanic rocks of the Quaternary East Eifel volcanic field, Germany, *Phys. Earth Planet. Inter.*, **94**, 23-41, 1996.
- Schnepp, E., and H. Hradetzky, Combined paleointensity and ⁴⁰Ar/³⁹Ar age spectrum data from volcanic rocks of the West Eifel field (Germany): Evidence for an early Brunhes geomagnetic excursion, *J. Geophys. Res.*, **99**, 9061-9076, 1994.
- Schweitzer, C., and H.C. Soffel, Palaeointensity measurements on postglacial lavas from Iceland, *J. Geophys.*, **47**, 57-60, 1980.
- Sharp, W. D., B. D. Turrin, P. R. Renne, and M. A. Lanphere, The ⁴⁰Ar/³⁹Ar and K/Ar dating of lavas from the Hilo 1-km core hole, Hawaii Scientific Drilling Project, *J. Geophys. Res.*, **101**, 11607-11616, 1996.
- Stolper E. M., D. J. DePaolo, and D. M. Thomas, Introduction to special

- section: Hawaii Scientific Drilling Project, *J. Geophys. Res.*, *101*, 11593-11598, 1996.
- Tanaka, H., Paleointensity high at 9000 years ago from volcanic rocks in Japan, *J. Geophys. Res.*, *95*, 17517-17531, 1990.
- Tanaka, H., and M. Kono, Preliminary results and reliability of paleointensity studies on historical and ¹⁴C dated Hawaiian lavas, *J. Geomagn. Geoelectr.*, *43*, 375-388, 1991.
- Tanaka, H., A. Otsuka, T. Tachibana, and M. Kono, Paleointensities for 10-22 ka from volcanic rocks in Japan and New Zealand, *Earth Planet. Sci. Lett.*, *122*, 29-42, 1994.
- Thellier, E., and O. Thellier, Sur l'intensité du champ magnétique terrestre dans le passé historique et géologique, *Ann. Géophys.*, *15*(3), 285-376, 1959.
- Tric, E., J. P. Valet, P. Y. Gillot, and I. Lemeur, Absolute paleointensities between 60 and 160 kyrs B. P. from Mount Etna, Sicily, *Phys. Earth Planet. Inter.*, *85*, 113-129, 1994.
- Valet, J. P., J. Brassart, I. Le Meur, V. Soler, X. Quidelleur, E. Tric, and P. Y. Gillot, Absolute paleointensity and magnetomineralogical changes, *J. Geophys. Res.*, *101*, 25029-25044, 1996.
- Vandamme, D., and M. Bruneton, Problem of elimination of directional data clusters in PSV studies, *Ann. Geophys.*, *16*, suppl. I, C208, 1998.
- Worm, H. U., A link between geomagnetic reversals and events and glaciations, *Earth Planet. Sci. Lett.*, *147*, 55-67, 1997.

C. Kissel and C. Laj, Laboratoire des Sciences du Climat et de l'Environnement, CEA-CNRS, 91198 Gif-sur-Yvette Cedex, France. (laj@lsce.cnrs-gif.fr)

(Received August 5, 1998; revised February 27, 1999; accepted March 11, 1999)